

JGR Atmospheres

RESEARCH ARTICLE

10.1029/2020JD033049

Special Section:

Water-energy-carbon fluxes over terrestrial water surfaces

Key Points:

- The MEP model is generalized for simulating surface water vapor fluxes over the lifecycle of the snowpack using Fluxnet data
- Two hypotheses are tested during the transition periods (snow melting and early growing seasons): (1) sublimation becomes negligible during snowmelt when snowpack is isothermal (0°C) and (2) transpiration is progressively activated as a function of air temperature during vegetation awakening
- The effectiveness of the MEP-ET model was confirmed through testing the hypotheses

Correspondence to:

I. Hajji, islem.hajji.1@ulaval.ca

Citation:

Hajji, I., Nadeau, D. F., Music, B., Anctil, F., & Wang, J. (2021). Analysis of water vapor fluxes over a seasonal snowpack using the maximum entropy production model. *Journal of Geophysical Research: Atmospheres*, 126, e2020JD033049. https://doi. org/10.1029/2020JD033049

Received 11 MAY 2020 Accepted 26 NOV 2020

© 2020. American Geophysical Union. All Rights Reserved.

Analysis of Water Vapor Fluxes Over a Seasonal Snowpack Using the Maximum Entropy Production Model

Islem Hajji¹, Daniel F. Nadeau¹, Biljana Music^{1,2}, François Anctil¹, and Jingfeng Wang³

¹Department of Civil and Water Engineering, Université Laval, Québec, QC, Canada, ²Ouranos - Consortium on Regional Climatology and Adaptation to Climate Change, Montréal, QC, Canada, ³School of Civil and Environmental Engineering, Georgia Institute of Technology, Atlanta, GA, USA

Abstract Snow cover plays a key role in the water and energy budgets over cold regions. Understanding and parameterizing water and heat exchange over snow surfaces in hydrologic models remains a major challenge. An innovative approach based on the theory of maximum entropy production (MEP) was developed for modeling energy budgets for snow-covered surfaces. This study generalizes the MEP model to simulate surface water vapor (latent heat) fluxes over an entire snowpack lifecycle, including snow accumulation and melting during the early growing season. The expanded MEP model combines soil evaporation, canopy transpiration, and snow sublimation to evaluate snow water loss during the lifecycle of the snowpack. Two hypotheses are tested: (1) sublimation becomes negligible during snowmelt when snowpack is isothermal (0°C) and (2) transpiration is progressively activated as a function of the air temperature during vegetation awakening. The proposed approach is shown to be effective for modeling the total surface water vapor fluxes over the snowpack's lifecycle. Both the hypotheses are supported by field observations.

1. Introduction

The Earth's surface in cold regions is usually covered with snow for several months of the year, if not yearround. As a result, snow plays a major role in the surface energy and water budgets in cold regions. Given its low-thermal conductivity and high-surface albedo, snow strongly affects the surface energy budget by altering the soil and atmospheric thermal regimes (e.g., Chen et al., 2014a; Clark & Serreze, 2000; Ge & Gong, 2009; Jin et al., 2006; Xu & Dirmeyer, 2011). Snow cover in cold regions also has a strong impact on the water cycle (Lehning, 2013) as snowmelt produces a large fraction of annual runoff. Snowmelt generates more than 70% of the annual streamflow in the Rocky Mountains (Stewart et al., 2004), between 50% and 80% of the annual runoff in the Canadian Prairies (Fang & Pomeroy, 2007; Gray et al., 1989), and between 40% and 60% in the northern hardwood forests of Canada (Essery et al., 2009; Hetherington, 1987). In the boreal biome, annual peak runoff, maximum soil moisture, and seasonal wetland recharge are all dependent on the spring snowmelt (Elliot et al., 1998; Pomeroy & Granger, 1997). Given the impact of snow cover on the Earth's system, there is an increasing demand for effective modeling of its interactions with the atmosphere. Over the past decades, efforts have been devoted to the development of snowpack models to support hydrological forecasting (e.g., Bernhardt et al., 2010; Feng et al., 2008; Lehning et al., 2006; Liston & Elder, 2006; Magnusson et al., 2015; Rutter et al., 2009), numerical weather forecasts, and climate modeling (e.g., Durand et al., 2009). These efforts have led to a variety of snowpack models ranging from conceptual single-layer bulk models to physically based multilayer models. Comparison studies of these models have been conducted to link their performance to the model structure and physics (e.g., Essery et al., 2013; Rutter et al., 2009; Slater et al., 2001). These studies have revealed large contrasts in the simulation of annual runoff over the seasonal snow cover period, mostly due to differences in the parameterization of latent heat fluxes, particularly sublimation (Andreadis et al., 2009; Barlage et al., 2010; Chen et al., 2014b; Slater et al., 2001). Substantial discrepancies in sublimation estimates confirm the importance of accurately representing the turbulent heat fluxes in modeling seasonal snowpack, especially during long snow accumulation phases (Chen et al., 2014b; Marks et al., 2002). Therefore, an accurate estimation of the latent heat fluxes over snow is crucial for snow hydrologic models.

HAJJI ET AL. 1 of 20



Several studies have attempted to quantify sublimation using field observations or model simulations for different regions of the world (Mott et al., 2018). Previous studies have suggested that snow sublimation during winter periods varies between 0.1% and 90% of the total snowfall depending on geographical locations, meteorological conditions, and model complexity (Groot Zwaaftink et al., 2013; MacDonald et al., 2010; Strasser et al., 2008). Sublimation was estimated at 0.36 mm d⁻¹ in continental Sweden (Bengtsson, 1980) and 1-2 mm d⁻¹ in the eastern Canadian Rocky Mountains (Golding, 1978). A total of 15% of snowfall was found to be lost through sublimation in the alpine regions (Hood et al., 1999; Kattelmann & Elder, 1991; Marks et al., 1992), whereas this fraction was 20% in the Atlas Mountains (Boudhar et al., 2016). Higher rates of sublimation were observed along the edge of the Eurasian cryosphere in Mongolia at the beginning and end of the snow-covered periods, especially under strong wind conditions (Zhang et al., 2008). Sublimation could reach 70% of the annual snowfall at wind-exposed locations in a mountainous region of southeastern Germany (Strasser et al., 2008). The progress in monitoring and modeling sublimation was hampered by difficulties in field observations of latent heat fluxes over snow surfaces, especially over complex terrain (Prueger et al., 1998). The total water vapor flux (ET) or associated latent heat flux (λ ET, with the latent heat of sublimation/evaporation λ) under partly snow-covered and heterogeneously vegetated terrain consists of soil evaporation, snow sublimation, and vegetation transpiration. Since latent heat fluxes during wintertime are relatively small compared with the other seasons, common ET models mainly focus on the snow-free seasons. Snow ET is commonly estimated using bulk transfer models, which relate water vapor fluxes to the corresponding scalar-gradients with wind speed and surface-roughness-dependent transfer coefficients. The major difficulties of the bulk transfer models are mainly caused by the need for two-level atmospheric humidity data, which are often not available over complex terrain in remote areas. Parameterization of the transfer coefficients under stable atmospheric conditions, which often prevail over snow surfaces, is challenging. Fitzpatrick et al. (2017) assessed the performance of the bulk transfer models of turbulent heat fluxes over a mid-latitude glacier during one melting season. They showed good agreement between the observed and estimated heat fluxes, but found that this approach was sensitive to atmospheric conditions and roughness lengths. Schlögl et al. (2017) showed that the stability corrections used in the bulk transfer models need to be improved for large temperature gradients and wind speed. Radic et al. (2017) also found that the bulk transfer model overestimates the turbulent heat fluxes. Therefore, alternative ET models for snow-covered surfaces are desirable.

A new model, referred to hereafter as MEP-E_{snow} model based on the theory of maximum entropy production (MEP; Wang et al., 2014), has been developed for simulating latent heat (water vapor) fluxes over snow and ice surfaces. The MEP theory as a selection criterion for non-equilibrium systems has been applied successfully in many fields (e.g., Dewar et al., 2006; Franklin et al., 2012; Lorenz et al., 2001; Malkus, 2003; Ozawa et al., 2001; Paltridge, 1978). The MEP principle applied to non-equilibrium thermodynamic systems offers an alternative approach to finding a solution by selecting the most likely partition of net radiation into evapotranspiration (ET) and heat flux among all possibilities allowed by the conservation of energy (Wang & Bras, 2011; Wang et al., 2014). Compared with other approaches, the MEP-E_{snow} model predicts latent heat fluxes (sublimation) without using wind speed, surface roughness, and aerodynamic resistances in bulk flux formulae. One major advantage of the MEP-E_{snow} model is that it requires only two input variables: net radiation and snow surface temperature, where the water vapor right above the snow (water/ice) surface is often assumed to be saturated. The thermal inertia of turbulent latent and sensible heat fluxes (not shown here), characterizing the boundary layer turbulent transport of water vapor and heat, are parameterized by implicitly taking into account the effect of wind speed, roughness, and aerodynamic resistance (Wang et al., 2010). More importantly, the MEP-E_{snow} model always satisfies the conservation of energy. More details about the MEP-E_{snow} model are given in Wang et al. (2014). The MEP-E_{snow} model has been validated (Wang et al., 2014) at a full snow cover site during the period of snow accumulation. More tests are desirable to evaluate its performance under more general conditions of snow-vegetation cover. Note that the MEP models of soil evaporation (MEP-E_v) and canopy transpiration (MEP-T_r; Wang & Bras, 2011) have been extensively validated over homogeneous terrain (e.g., Shanafield et al., 2015; Wang et al., 2017). Hajji et al. (2018) recently generalized MEP models (MEP-E_v and MEP-T_r) to estimate ET over heterogeneous surfaces with variable vegetation cover and water stress using a vegetation coefficient for improving the simulations of soil evaporation and canopy transpiration. Their analysis confirmed the effectiveness of the

HAJJI ET AL. 2 of 20



MEP model under conditions of zero to moderate water stress by introducing a soil-moisture-dependent water stress function.

To our knowledge, the physical process of ET over partially vegetated surfaces in the presence of seasonal snow cover is not fully understood. Moreover, the performance of the MEP model for estimating latent heat flux under the conditions when (soil) evaporation, transpiration, and sublimation may coexist has not been evaluated. It is well understood that snow accumulation and melting, as well as plant phenological cycles, play essential roles in water vapor transfer into the atmosphere (Wang et al., 2013). Both the energy and moisture regimes during the transition periods between the cold (snow) and warm (snow-free) seasons drive the water vapor transfer. The objective of this study is to develop a framework for the simulation of total water vapor flux over the lifecycle of a snowpack, including snow accumulation and snowmelt in the early growing seasons, and to evaluate its performance under various geographical and climatic conditions.

The paper is organized as follows: Section 2 briefly describes the MEP-ET model (Wang & Bras, 2011; Wang et al., 2014), highlighting its formulae for the cases of soil, canopy, and snow surfaces. Section 3 presents the hypotheses for two scenarios of snow conditions characterizing the transition from the cold to the warm season. Section 4 describes the study sites and input data. Section 5 presents the findings.

2. MEP Model Formulation

The MEP model provides a unique method of partitioning net radiation, R_n , into surface heat fluxes (latent λET , sensible H and ground/snow heat flux Q) for various types of land covers (Wang & Bras, 2011; Wang et al., 2014). The MEP formulation of λET , H, and Q for soil, canopy, and snow surface is expressed as follows:

$$\begin{cases}
H \left[1 + B(\sigma) + \frac{B(\sigma)}{\sigma} \frac{I_{s}}{I_{0}} |H|^{-\frac{1}{6}} \right] = R_{n} \\
\lambda ET = B(\sigma)H
\end{cases}$$
(1)

with the following surface energy balance equations:

$$R_{\rm n} - \lambda ET - H = \begin{cases} Q, & \text{nonvegetated surfaces} \\ 0, & \text{vegetated surfaces} \end{cases},$$

$$Q + R_{\rm ns}, & \text{snow/ice surfaces}$$
(2)

where R_n and R_{ns} are the net radiation and net solar radiation, respectively, I_s is the thermal inertia of the soil/snow material, and I_0 is the apparent thermal inertia of the air (see Equation 3 of Wang & Bras, 2011). $B(\sigma)$ is the inverse of the Bowen ratio:

$$B(\sigma) = 6\left(\sqrt{1 + \frac{11}{36}\sigma} - 1\right) \text{ with } \sigma(T_s, q_s) \equiv \eta_s \frac{\sqrt{\alpha \lambda^2}}{c_p R_v} \frac{q_s}{T_s^2}$$
(3)

where σ is a dimensionless parameter as a function of surface temperature $(T_s(K))$ and surface-specific humidity $(q_s(kg kg^{-1}))$. In Equation 3, c_p is the specific heat of the air at constant pressure $(J kg^{-1} K^{-1})$, R_v is the gas constant of water vapor $(J kg^{-1} K^{-1})$, λ is the latent heat of vaporization of liquid water or sublimation of solid water $(J kg^{-1})$, α is the ratio of the eddy diffusivities for water vapor and heat (taken as one here), and η_s is the water stress factor representing the relative plant water availability defined in Hajji et al. (2018). Since the natural landscape is often covered with bare soil, canopy, and snow with time-varying proportions, the MEP formulae for the three types of land covers need to be used simultaneously.

HAJJI ET AL. 3 of 20

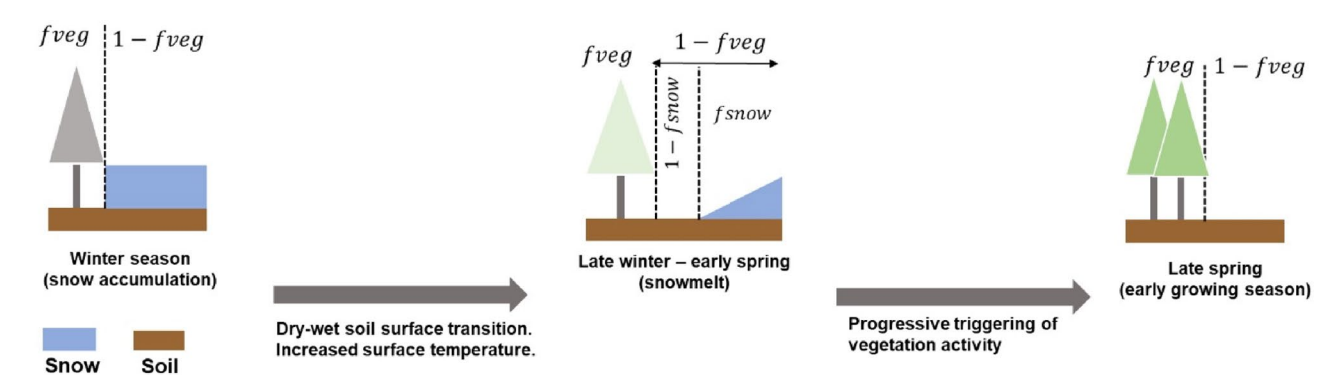


Figure 1. The change in snow and vegetation cover during snow accumulation and melting period.

2.1. MEP Implementation for ET Estimation (MEP-ET) Over the Lifecycle of a Snowpack

The total ET consists of soil evaporation, canopy transpiration, and snow sublimation. Each component of ET varies with the biological and environmental conditions. For the case of coniferous forests located in the cold regions considered in this study, most plants are in dormancy and do not contribute to ET during the winter, while transpiration dominates during the summer when energy and water are abundant. Figure 1 illustrates snow and vegetation cover change during the winter-spring-summer transition period. According to previous observational studies of coniferous canopies, snow is the main local source of atmospheric water vapor during winter (Harding & Pomeroy, 1996; Nakai et al., 1999). The total surface water vapor flux into the atmosphere is expressed as

$$ET = \beta f_{\text{snow}} \left(1 - f_{\text{veg}} \right) E_{\text{snow}} - \left(1 - f_{\text{snow}} \right) \left(1 - f_{\text{veg}} \right) E_{\text{v}} + f_{\text{veg}} T_{\text{r}}, \tag{4}$$

where β (0 or 1) is an indicator of snow sublimation (see Section 3.2), E_{snow} , E_{v} , and T_{r} the MEP modeled snow sublimation, soil evaporation, and transpiration, respectively, f_{snow} the fractional snow cover, and f_{veg} the fractional canopy cover. In this study, f_{veg} is parameterized following Wittich and Hansing (1995) as

$$f_{\text{veg}} = \frac{\text{NDVI} - \text{NDVI}_{\text{min}}}{\text{NDVI}_{\text{max}} - \text{NDVI}_{\text{min}}},$$
(5)

where NDVI is the Normalized Difference Vegetation Index, and $NDVI_{max}$ and $NDVI_{min}$ are its values for dense vegetation and bare soil, respectively. The fractional snow cover may be parameterized as a nonlinear function of snow depth (Liston, 2004; Niu & Yang, 2007). During the snowmelt period, this parameterization tends to overestimate the snow fraction (Niu & Yang, 2007; Su et al., 2008). Therefore, a modified parameterization of snow fraction based on snow depth and snow density (Niu & Yang, 2007) is used in this study as

$$f_{\text{snow}} = \begin{cases} 1, & T_{\text{snow}} < 0 \text{ (snow accumulation)} \\ \tanh \left(\frac{d_{\text{s}}}{2.5z_0 \left(\rho_{\text{s,old}} / \rho_{\text{s,new}} \right)^m} \right), & T_{\text{snow}} = 0 \text{ (snowmelt)} \end{cases}$$
(6)

where d_s is the snow depth (m), T_{snow} the snow surface temperature, z_0 (= 0.01 m) the surface roughness, $P_{(s,old)}$ and $P_{(s,new)}$ old and fresh snow density, and m an empirical coefficient. Niu and Yang (2007) tested Equation 6 using long-term (1979–1996) ground-based snow depth data from North America (Brown et al., 2003) and satellite-derived monthly f_{snow} , with a focus on larger river basins. Using the same database, Su et al. (2008) obtained optimal values of the model parameters in Equation 6 for different landscape categories, including the boreal biome used in this study: $P_{(s,old)} = 500 \text{ kg m}^{-3}$, $P_{(s,new)} = 100 \text{ kg m}^{-3}$, and

HAJJI ET AL. 4 of 20

m = 2.23. Note that during the snow accumulation period ($T_{\rm snow} < 0$), $f_{\rm snow}$ is assumed to be 1, since ET during this period is dominated by sublimation.

2.2. Low Temperature Constraint on Canopy Transpiration

Variations of snowpack and vegetation cover strongly affect canopy transpiration (Betts, 2011), especially during the early growing season. Increasing net radiation due to declining albedo results in rising canopy temperature, which in turn leads to higher atmospheric evaporation demand in favor of canopy transpiration (Kelly & Goulden 2016; Liu et al., 2016; Monson et al., 2005; Wieser & Tausz, 2007; Winchell et al., 2016).

Numerous studies focusing on cold forested regions have shown that canopy transpiration and photosynthesis rates during transition from the dormant to active vegetation periods are strongly dependent on the temperature (Mellander et al., 2006; Monson et al., 2005). Cold-temperature-induced inhibitory effects on photosynthesis and transpiration in forest ecosystems have been well documented (Bergh & Linder, 1999; Liu et al., 2016; Mellander et al., 2006). For instance, Mellander et al. (2006) showed that low soil temperature during the spring-early summer reduced transpiration of Scots pines in Sweden using a coupled heat and mass transfer model for the soil-plant-atmosphere system (COUP model). Later, Mellander et al. (2008) suggested that air and soil temperatures must be considered when estimating the rate of gas exchange (transpiration and photosynthesis) of boreal environments. Repo et al. (2008) showed that frozen soils effectively blocked the water uptake and trunk sap flow (transpiration) of Scots pine saplings. Below ground water transfer is often limited by low soil water (liquid) content due to freezing. Low soil temperature reduces the soil and plant hydraulic conductance and water uptake (e.g., Kramer & Boyer, 1995). In early spring, low soil and air temperature reduce the water uptake, and hence transpiration and photosynthesis (Kozlowski et al., 1991). Mellander et al. (2004) and Wang et al. (2018) found that soil temperature below 8°C, which is common in spring in the northern boreal biome, restricts transpiration as a result of low stomatal conductance and, likely, lower root permeability. Bergh and Linder (1999) found that sap flow (transpiration) was greatly reduced when the ground was covered with snow and soil temperature was close to freezing point.

Considering the aforementioned phenomena, the MEP model needs to be configured for the beginning of the growing season. A recent study (Hajji et al., 2018) proposed an empirical coefficient in the MEP- T_r model to account for soil water availability for transpiration during dry spells. To account for the effect of cold temperatures on transpiration, the following empirical function $m(T\min)$ is proposed in the MEP- T_r model:

$$m(T\min) = \begin{cases} 1, & T\min_{\text{open}} \\ \frac{T\min - T\min_{\text{close}}}{T\min_{\text{open}} - T\min_{\text{close}}}, & T\min_{\text{close}} < T\min < T\min_{\text{open}}, \\ 0, & T\min_{\text{close}} \end{cases}$$
(7)

where Tmin is the daily minimum air temperature, and Tmin_{open} and Tmin_{close} are the threshold values of Tmin. When Tmin is lower than Tmin_{close}, stomata close almost completely, halting canopy transpiration. On the contrary, when Tmin exceeds Tmin_{open}, stomata are fully open. The values of Tmin_{open} and Tmin_{close} for the range of studied biomes are taken from Mu et al. (2007). Following Hajji et al. (2018), σ in Equation 3 is reformulated as

$$\sigma(T_{ls}, q_{ls}, \eta_s) = m(T_{min}) \eta_s \frac{\sqrt{\alpha \lambda^2}}{c_p R_v} \frac{q_{ls}}{T_{ls}^2}$$
(8)

where all the variables are defined as in Equation 3.

HAJJI ET AL. 5 of 20



2.3. Modeling Sublimation During Snowmelt (β Coefficient)

The isothermal (or ripe) condition (uniform 0°C snow temperature) is observed during snowmelt (e.g., DeWalle & Rango, 2008). Theoretically, the net radiative energy at the snow surface can be used for both melting and sublimation depending on, among other factors, the atmospheric vapor demand. During the snowmelt season in spring, net radiation is considered to be the main source of energy for melting. Numerous studies have attempted to quantify sublimation during snowmelt. For instance, Harding (1986) and Kuusisto (1986) have found that sublimation represents a small fraction of the snowpack energy budget during melting. Martinelli (1960) reported that sublimation accounted for only 2% of the snowpack ablation (sublimation + melt) in the Rocky Mountains. Likewise, van den Broeke et al. (2008), who investigated several sites in western Greenland, have found that sublimation during snowmelt was rather small (<10 W m⁻²). Spring latent heat fluxes over snow surfaces are also reported to be limited (Lee, 2004; Link & Marks, 1999). Some studies have reported non-negligible sublimation during snowmelt. Beaty (1975) found that sublimation was responsible for 60% of the spring ablation in the White Mountains of California. Jackson and Prowse (2009) reported that sublimation was continuous during the melting phase with rates of about 0.4 mm d⁻¹ in southern British Columbia. Stiegler et al. (2016) demonstrated that water loss through sublimation reached 8.6 mm during the entire spring snowmelt (17 days) at a wet and exposed site in northeastern Greenland. Schulz and de Jong (2004) showed that strong solar radiation and high air temperatures over semiarid regions supported high sublimation rates for long periods, provided that the snowpack remained cold and snowmelt did not dominate snow ablation. In the Mediterranean mountains, sublimation was reported at 20% of the total snowpack ablation (Jepsen et al., 2012). Zhou et al. (2012) studied sublimation in different stages of snow cover (the cumulative, stable, and melting stages) and found that the average daily sublimation during the melting stage was greater than that during the cumulative and stable stages. Overall, all these past studies suggest that the sublimation rates during snowmelt may vary depending on the geographical and meteorological conditions.

In this study, the total ET, including sublimation, over a seasonal snowpack is simulated using the MEP model according to Equations 1–8. As mentioned above, β is introduced to control the occurrence of sublimation during snowmelt periods (see Equation 4): sublimation is turned on when $\beta=1$ and it is turned off when $\beta=0$. The sensitivity of the MEP-ET model to β is evaluated by comparing the modeled water vapor fluxes with the field observations.

2.4. Model Evaluation Criteria

The performance of the MEP-ET model was evaluated using the following metrics: the Kling-Gupta efficiency (KGE; Gupta et al., 2009), the mean bias (MB) index, and the root mean square error (RMSE) as follows:

KGE =
$$1 - \sqrt{(cc - 1) + (a - 1) + (b - 1)}$$

$$MB = \frac{\sum_{i=1}^{n} ET_{est}, i}{\sum_{i=1}^{n} ET_{obs}, i}$$

RMSE =
$$\sqrt{\frac{1}{n}\sum_{i=1}^{n} \left(ET_{est,i} - ET_{obs,i}\right)^2}$$

where $\mathrm{ET}_{\mathrm{est},i}$ and $\mathrm{ET}_{\mathrm{obs},i}$ are the estimated and observed hourly or daily ET time series, n is the length of the time series, $\mathrm{ET}_{\mathrm{obs}}$ is the mean value of observations, cc is the linear correlation coefficient between $\mathrm{ET}_{\mathrm{obs}}$ and $\mathrm{ET}_{\mathrm{est}}$, a is the measure of variability in the data values (equal to the ratio of standard deviation of $\mathrm{ET}_{\mathrm{est}}$ to that of $\mathrm{ET}_{\mathrm{obs}}$), and b is the ratio of mean $\mathrm{ET}_{\mathrm{est}}$ to mean $\mathrm{ET}_{\mathrm{obs}}$. MB values less or greater than one signify an overall underestimation or overestimation by the MEP model over the test periods. Good model performance is in-

HAJJI ET AL. 6 of 20

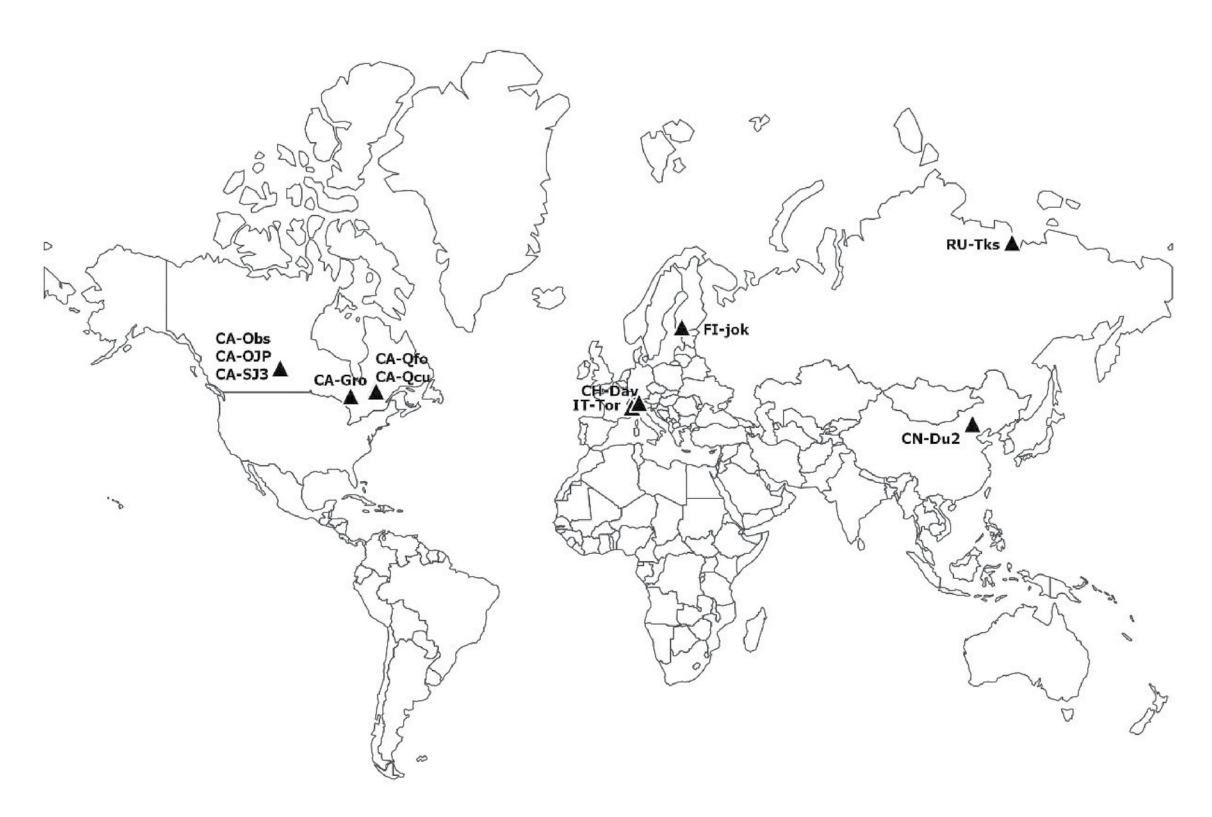


Figure 2. Location of the selected study sites.

dicated by KGE values approaching 1, while values less than 0 indicate a model performance inferior to the mean observation (\overline{ET}_{obs}) at all-time steps. RMSE provides a measure of differences between the observed and simulated ET.

3. Case Study

3.1. Study Sites

Eddy covariance (EC) observations over snow-covered forests have become increasingly available (e.g., Arck & Scherer, 2002; Marks et al., 2008; Molotch et al., 2007; Nakai et al., 1999; Parviainen & Pomeroy, 2000; Pomeroy & Granger, 1997) and are now commonly used in snow studies (Gryning et al., 2001; Harding & Pomeroy, 1996; Molotch et al., 2007; Nakai et al., 1999; Pomeroy & Essery, 1999; Reba et al., 2012; Sexstone et al., 2016; Turnipseed et al., 2002, 2003). In this analysis, FLUXNET (http://fluxnet.ornl.gov/) data were used to evaluate the MEP model for simulating ET over the snowpack's lifecycle. FLUXNET provides half-hourly EC fluxes and meteorological variables needed for our analyses. Eleven sites in Canada, Finland, Russia, Italy, Switzerland, and China (Figure 2) are selected in this study, one per country except for Canada, due to data availability. Six Canadian boreal forest sites were chosen across three provinces (Saskatchewan, Quebec, and Ontario).

The selected Fluxnet sites are from different biomes (Table 1): grassland (GRA) such as CN-Du2, IT-Tor and Ru-Tks sites, cropland (CRO), as FI-jok site and mixed (MF), and evergreen needleleaf (ENF) forests with diverse climatic conditions. For example, the Russian site (Ru-Tks) is characterized by a cold subarctic climate (Dfd) with annual mean temperature lower than -12° C and 235 snow cover days. The Chinese site (CN-Du2) has a monsoon humid continental climate (Dwb) with cold and dry winter. The climate of Canadian sites varies from semiarid subarctic in Saskatchewan (annual precipitation less than 400 mm and annual temperature close to 0° C) to humid subarctic in Quebec (annual precipitation greater than 900 mm and lower annual temperature; Table 1. Logistic difficulties of field experiments due to snow deposition on

HAJJI ET AL. 7 of 20



Table 1 <i>Main Characteristics</i>	of the Study Sites							
			Elevation	Veg	Vonnen	Mean annual	Mean annual	

			Elevation	Veg.	Koppen	Mean annual temp.	Mean annual precip.		Height measure
Site	Location	Lat (°N), Lon. (°E)	(m)	Type	climate	(°C)	(mm)	Years	(m)
CA-Obs	Saskatchewan—Canada	53.99, -105.12	629	ENF	Dfc	0.8	406	2004-2007	(1, 6)
CA-OJP	Saskatchewan—Canada	53.91, -104.69	579	ENF	Dfc	0.1	431	2006-2010	(1, 16, 10, 5)
CA-SJ3	Saskatchewan—Canada	53.87, -104.64	495	ENF	Dfc	0.13	433	2005-2006	(1, 4)
CA-Gro	Ontario—Canada	48.22, -82.16	340	MF	Dfb	1.3	831	2006-2012	(1.5, 18, 11)
CA-Qfo	Quebec—Canada	49.69, -74.34	382	ENF	Dfc	-0.4	962	2006-2010	(1.5, 13)
CA-Qcu	Quebec—Canada	49.27, -74.04	392	ENF	Dfc	0.13	950	2009-2010	(1.6)
CN-Du2	Duolun—China	42.04, 116.28	1,350	GRA	Dwb	2.01	319	2006-2008	3
FI-jok	Jokioinen—Finland	60.89, 23.51	109	CRO	Dfc	4.6	627	2000	3
IT-Tor	Torgnon—Italy	45.84, 7.57	2,160	GRA	Dfc	2.9	920	2011-2012	3.5
Ru-Tks	Tiksi—Russia	71.59, 128.88	7	GRA	Dfd	-12.7	323	2012-2014	2.9
CH-Dav	Davos—Switzerland	46.81, 9.85	1,639	ENF	Dfb	2.8	1,062	2009-2010	X

sensors and limited site accessibility during winter are responsible for data gaps. The test periods are carefully selected with minimum missing data for the analysis.

3.2. Study Periods

To assess the performance of the MEP-ET model for the lifecycle of the snowpack, three critical periods were selected (Figure 3): (1) a winter accumulation period with a growing snowpack when the snow temperature is below the freezing point (0°C); (2) a spring snowmelt period with an isothermal snowpack and above freezing air temperatures and elevated soil moisture caused by melting snow; and (3) a spring-summer veg-

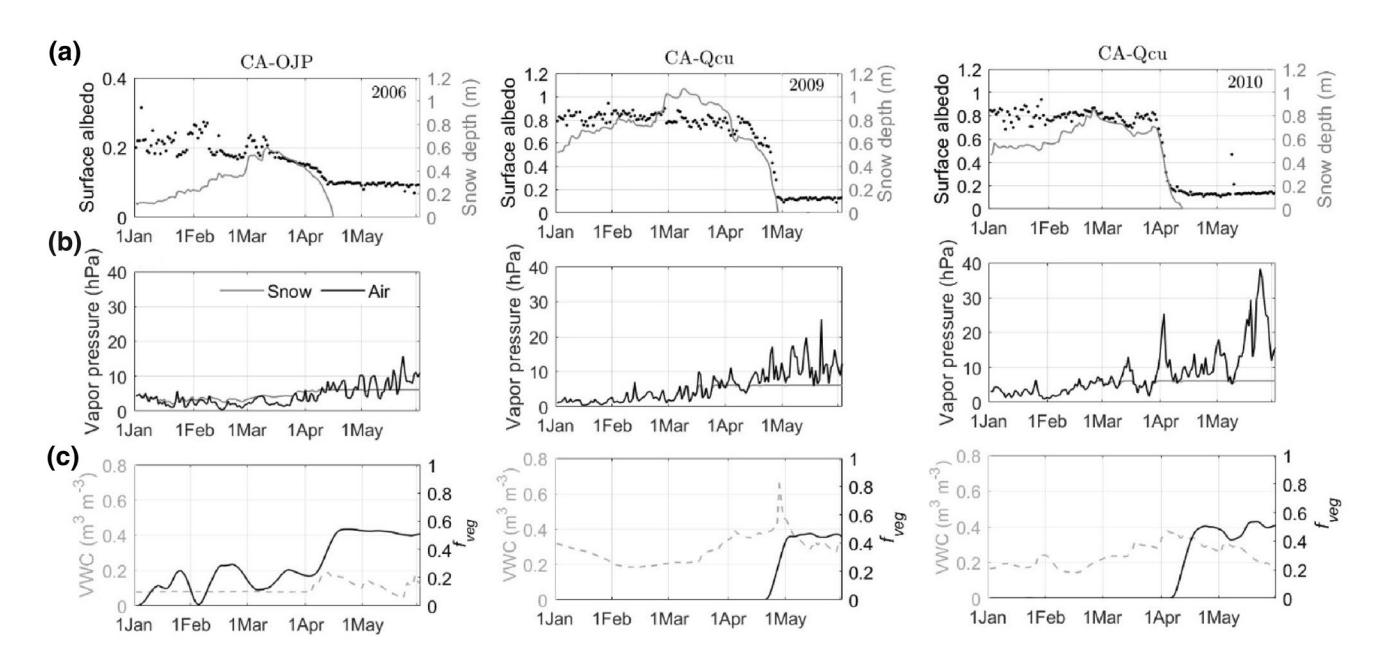


Figure 3. Daily meteorological variables at CA-OJP and CA-Qcu. (a) Snow surface albedo (black dots) at 12:00 local time (LT) and snow depth (gray curve); (b) near-surface air vapor pressure (black solid curve) and estimated snow vapor pressure using observed snow temperature at 12 LT (gray solid curve); and (c) volumetric snow water content (VWC, gray areas) and the fractional canopy cover vegetation, f_{veg} (black dots).

HAJJI ET AL. 8 of 20



etation awakening period when snowmelt ends and the growing season begins. Note that the early stage of snow accumulation period when f_{snow} varies from 0 to one is excluded in this study.

The CA-OJP and CA-Qcu sites have different seasonal cycles as shown in Figure 3. During the accumulation period, surface albedo reaches its maximum, then decreases as the snowpack melts to reach its annual minimum when snow vanishes. During the accumulation period, surface albedo is 0.9 at the CA-Qcu cleared forest site, 0.2 at the CA-OJP dense forest site, and 0.6 and 0.15, respectively, during snowmelt. At the cleared forest site, the ground may be completely covered with snow, while trees partially mask the snowpack below the canopy at the dense forested site. For the latter case, surface albedo is much lower as a result of the darker surface. The variability in snowpack depth for 2009 and 2010 at CA-Qcu is shown in Figure 3. The 2009 snowpack was deeper than in 2010; snowmelt also began and finished later than in 2010. A longer lasting snowpack increases albedo, leading to cooler near-surface temperatures. CA-OJP and CA-Qcu are not windy sites, where the mean winter wind speed was relatively low at 2.6 and 3.7 m $\rm s^{-1}$ at CA-OJP and CA-Qcu, respectively. Therefore, no major snow redistribution by wind is expected.

3.3. Input Data

Table 2 summarizes the data needed for testing the hypotheses and for evaluating the MEP model. Since snow surface-specific humidity is often assumed to be at the saturation level, only snow temperature (T_{snow}) and net

MEP model	Input	Definition	Comment
MEP-E _{snow}	$T_s \approx T_{\rm snow}$	Snow surface temperature (°C)	Measured
	$q_s \approx q_{\rm sat} \left(T_{\rm snow} \right)$	Saturation specific humidity (kg kg ⁻¹)	Computed
	$I_s \approx I_{\rm swi}$	Snow thermal inertia $\left(W m^{-2} K^{-1} s^{\frac{1}{2}}\right)$	Constant (Wang et al., 2014)
$MEP-E_{v}$	$T_s \approx T_{ss}$	Soil surface temperature (°C)	Air temperature measurements closest to the surface (\sim 2 m)
	$q_s \approx q_{ss}$	Soil specific humidity (kg kg ⁻¹)	Computed from closest to the surface air temperature and relative humidity measurements
	$I_s \approx I_{ss}$	Soil thermal inertia $\left(W m^{-2} K^{-1} s^{\frac{1}{2}}\right)$	Computed (Equation 8 in Wang et al., 2010)
MEP-T _r	$T_s \approx T_{ls}$	Leaf surface temperature (°C)	Air temperature measurements closest to the canopy top
	$q_s \approx q_{ls}$	Leaf specific humidity (kg kg ⁻¹)	Computed from air temperature and relative humidity measurements closest to the canopy top
	$I_s \approx 0$	Leaf thermal inertia $\left(W m^{-2} K^{-1} s^{\frac{1}{2}}\right)$	Neglected
MEP-ET	f_{veg}	Vegetation index	Equation 5 with $NDVI_{\text{max}} \approx 0.95$ and $NDVI_{\text{min}} \approx 0.05$
	f_{snow}	Snow fraction	Equation 6
	$\eta_{_{\mathrm{S}}}ig(T\mathrm{min}ig)$	Temperature stress factor	Equation 8; depending on the type of plants (MF or ENF, in this work). $ MF \left(T \min_{\text{close}} \mid T \min_{\text{open}} \right) \approx (0 \mid 9.50) $ $ ENF \left(T \min_{\text{close}} \mid T \min_{\text{open}} \right) \approx (0 \mid 8.31) $

HAJJI ET AL. 9 of 20

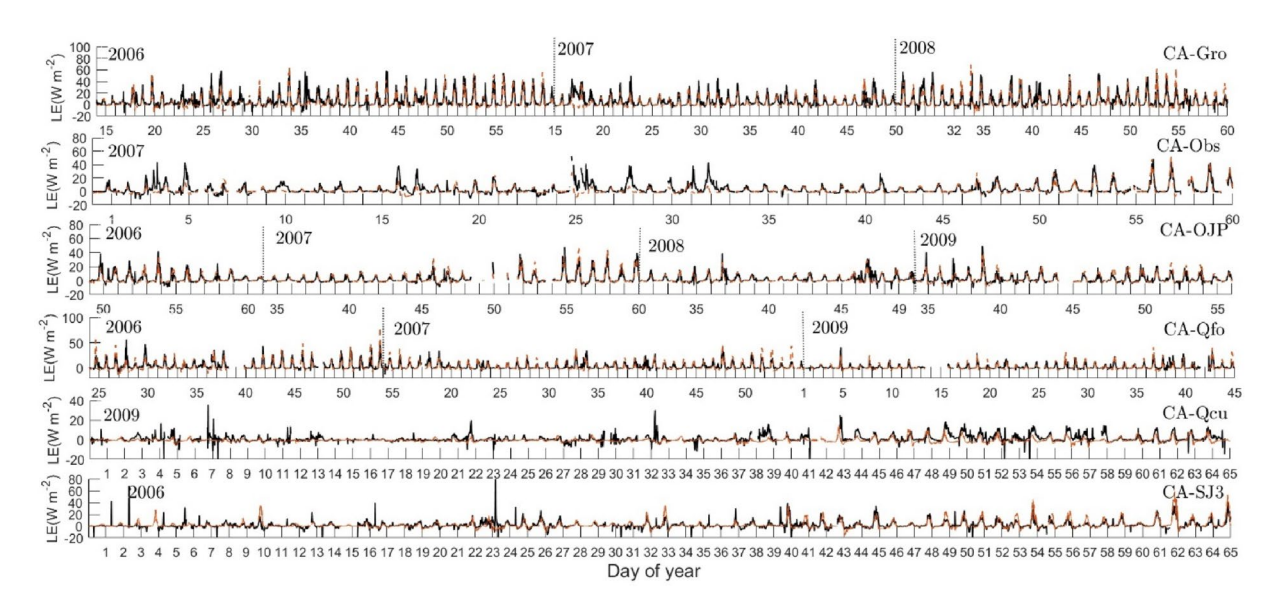


Figure 4. MEP-ET modeled versus observed water vapor (latent heat) flux during the snow accumulation periods at Canadian forest sites.

radiation (R_n) data are needed for the MEP-E_{snow} model. When snow temperature data were not available at the CA-Qcu and CA-Qfo sites, air temperatures at 1.6 and 1.5 m were used as a surrogate. The sensitivity of using air temperature as a surrogate for snow temperature in the simulation of sublimation by the MEP-E_{snow} model was analyzed using field observations at the four sites where both snow and air temperature data are available. Note that the air temperature used in the MEP-E_{snow} model was measured close to the ground (Table 1).

The MEP- T_r and MEP- E_v models require near-leaf/soil surface temperature and humidity data. Since they were often not available, observations closest to the canopy/soil surface were used instead. For example, since the canopy height at the CA-OJP site is 14 m, the leaf surface temperature and humidity were assumed equal to the air temperature and humidity averaged from two measurement heights (10 and 16 m). Soil temperatures measured at a 2-cm depth are used as the surrogate for soil surface temperature (T_{ss}). Soil-surface-specific humidity (q_{ss}) was taken as the air-specific humidity near the soil surface calculated from 2 m T_{ss} and relative humidity (RH) measurements using the well-known Clausius-Clapeyron equation. Net radiation, soil moisture, and snow depth were directly measured at the study sites.

In addition to the above data, snow and vegetation fractional covers f_{snow} , f_{veg} in Equation 4 are required to estimate the total ET, especially once the melting process starts. However, with the exception of Canadian

Table 3Performance Values of the MEP-ET Model With Statistics KGE, MB, and RMSE (W m⁻²) at Seven Study Sites During Snow Accumulation

. ,		7 0		
	KGE	MB	RMSE (W m ⁻²)	N
CA-OJP	0.68	0.83	6	3197
CA-Obs	0.76	1.07	5	1683
CA-Gro	0.69	0.99	10	6069
CA-Qfo	0.50	1.24	8	2077
CN-Du2	0.62	1.04	10.5	2132
FI-jok	0.38	1.3	5.8	572
CH-Dav	0.41	-0.33	40.35	1761

Note. N is the number of data points.

Abbreviations: KGE, Kling-Gupta efficiency; MB, mean bias; RMSE, root mean square error.

sites, f_{snow} , f_{veg} data are not available for the other sites (CH-Dav, Ru-Tks, IT-Tor, FI-jok, and CN-Du2) where the MEP model can only be evaluated for snow accumulation periods.

4. Results and Discussion

4.1. Snow Accumulation Period

Figures 4 and 5 compare hourly MEP-ET water vapor fluxes with observations at the study sites during the snow accumulation period only (i.e., as long as the snow is not ripe). The statistical metrics describing the performance of the MEP-ET model are presented in Table 3. The results of the statistical metrics of some sites (CA-SJ3, CA-Qcu, IT-Tor, and Ru-Tks) are not presented due to low data quality.

Overall, MEP-ET fluxes are in close agreement with observations. KGE values vary from 0.50 to 0.76 MB and from 0.83 to 1.24 MB. The agreement tends to be less close at night times when sublimation is underestimated

HAJJI ET AL. 10 of 20

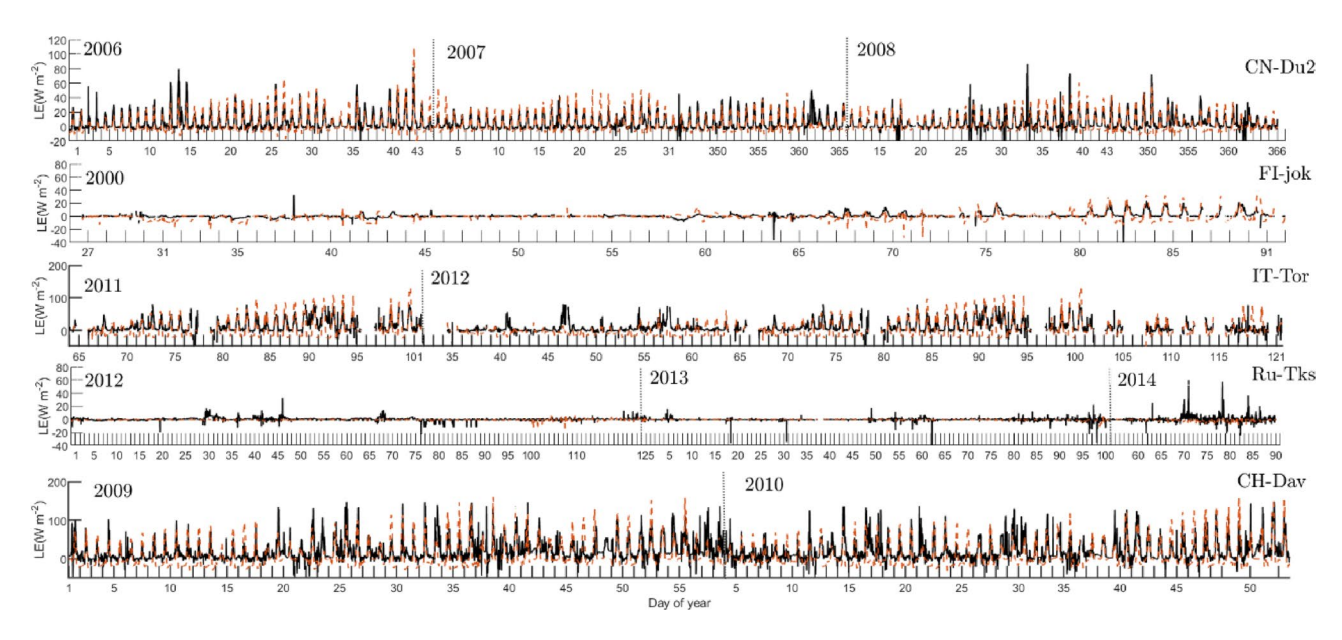


Figure 5. Same as Figure 4 for the CN-Du2, FI-Jok, IT-Tor, Ru-Tks, and CH-Dav sites.

at some sites (e.g., CA-Qcu, IT-Tor, and Ru-Tks). This is arguably due to the measurement errors of EC fluxes under stable nocturnal conditions (Marks et al., 2008). Therefore, the nighttime data are excluded in the calculation of the metrics (Table 3, Figure 11). The observed and estimated daily mean sublimation rates at the CA-OJP site from February 15 to March 12, 2006 (26 days) are 0.17 (max. 0.48) and 0.22 (max. 0.49) mm d⁻¹, respectively. CA-Gro observed and estimated sublimation rates reach 0.28 (max. 0.86) mm d^{-1} and 0.26 (max. 0.78) mm d^{-1} during the snow accumulation period (from January 10 to March 22, 2006). Sublimation at drier forest sites (CA-Obs, CA-OJP) was lower than at wetter sites (CA-Gro), a phenomenon captured by the MEP model. In addition, the observed and estimated daily mean sublimation rates at the humid open forest site CA-Qcu during accumulation (February 1–16, 2010) are 0.04 (max. 0.05) mm d⁻¹ and 0.02 (max. 0.05) mm d⁻¹, respectively. For the same period, much higher values have been obtained at the closer humid forest site CA-Gro, at 0.14 (max. 0.26 mm d⁻¹) for the observed sublimation rate and 0.17 (max. 0.23 mm d⁻¹). At cold and dry sites, such as Ru-Tks, the MEP-ET model accurately simulates the diminishing sublimation rates. Obviously, cold temperature limits sublimation during the winter months. Low sublimation rates during wintertime should not be considered negligible because of its importance in determining the water and energy balance over cold regions (Liston & sturm, 2004; Svoma, 2016). For example, in the Gurbantunggut Desert, low winter precipitation results in the sublimation of 24% of the snowfall (Svoma, 2016). At dryer grassland sites, such as CN-Du2, the observed and estimated daily mean sublimation rates are 0.18 (max. 0.47) mm d⁻¹ and 0.20 (max. 0.60) mm d⁻¹, respectively, for two winter months (January and February 2006). The observed and estimated sublimation rates at open sites (dry or humid) are always lower than those at closed forest sites, which contrasts with previous studies (Marks & Dozier, 1992; Jackson & Prowse, 2009) showing that ground sublimation from open sites is generally higher than for closed forested sites. In general, sublimation rates increase with the forest opening size, wind speed (increasing surface layer turbulence), and temperature (Bernier & Swanson, 1993; Schmidt et al., 1998). The open and closed sites of this study are not exposed to high wind speeds ($\leq 4 \text{ m s}^{-1}$). The above analysis confirms the effectiveness of the MEP model in modeling sublimation during snow accumulation at diverse (open and closed) forest sites.

4.2. Snowmelt Period

4.2.1. Sublimation During Snowmelt and No Criterion for Vegetation Awakening.

Figure 6 shows the MEP-ET modeled hourly latent heat (water vapor) fluxes during the snowmelt period with no constraint ($\beta = 1$ in Equation 4) at the Canadian sites. The original MEP-ET model ($\beta = 1$ in

HAJJI ET AL. 11 of 20

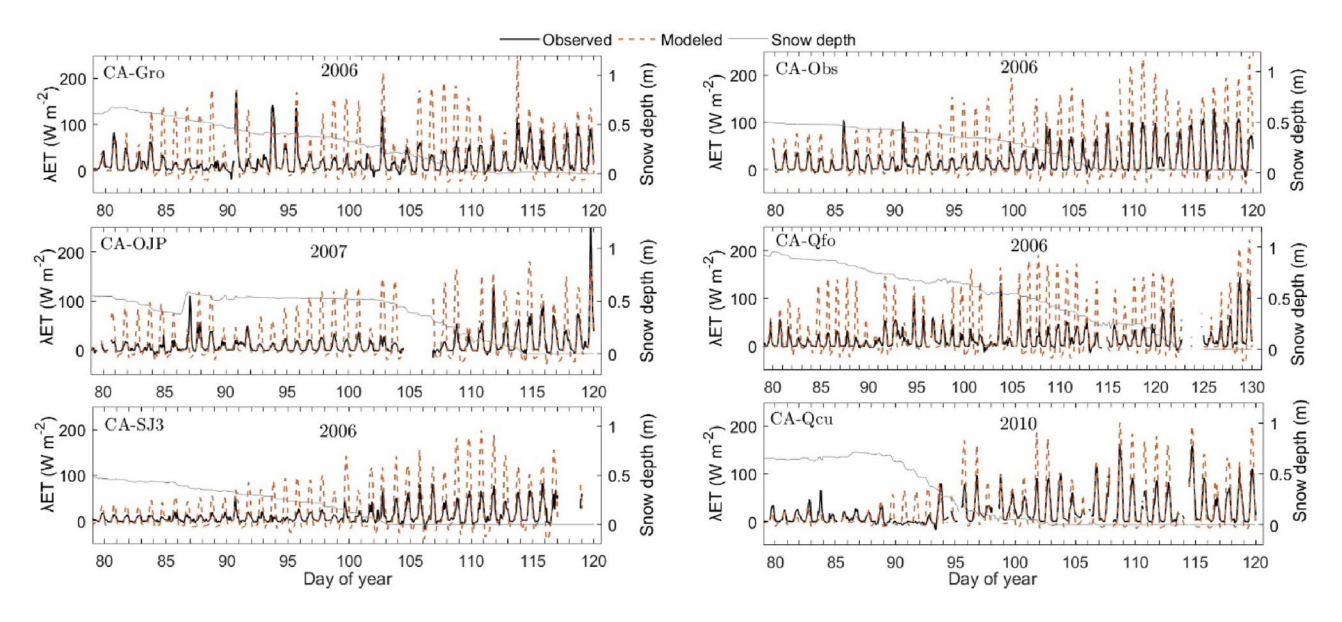


Figure 6. The original MEP-ET modeled ($\beta = 1$ in Equation 4) versus observed water vapor flux at Canadian forest sites.

Equation 4) overestimates water vapor fluxes assuming that sublimation continues during snowmelt in the early growing season. Figure 7 compares the simulated versus observed hourly MEP-ET water vapor fluxes assuming sublimation during the snowmelt period ($\beta = 1$ in Equation 4) for spring 2006 at the CA-OJP site. When the snow depth starts declining on day 75, the model predicts significant sublimation (>50 W m⁻²), which is inconsistent with the observations. Note also that transpiration starts when there is still ~40 cm of snow on the ground, again leading to an overestimation of latent heat fluxes in the final stage of the snowmelt period, as well as in the early growing season.

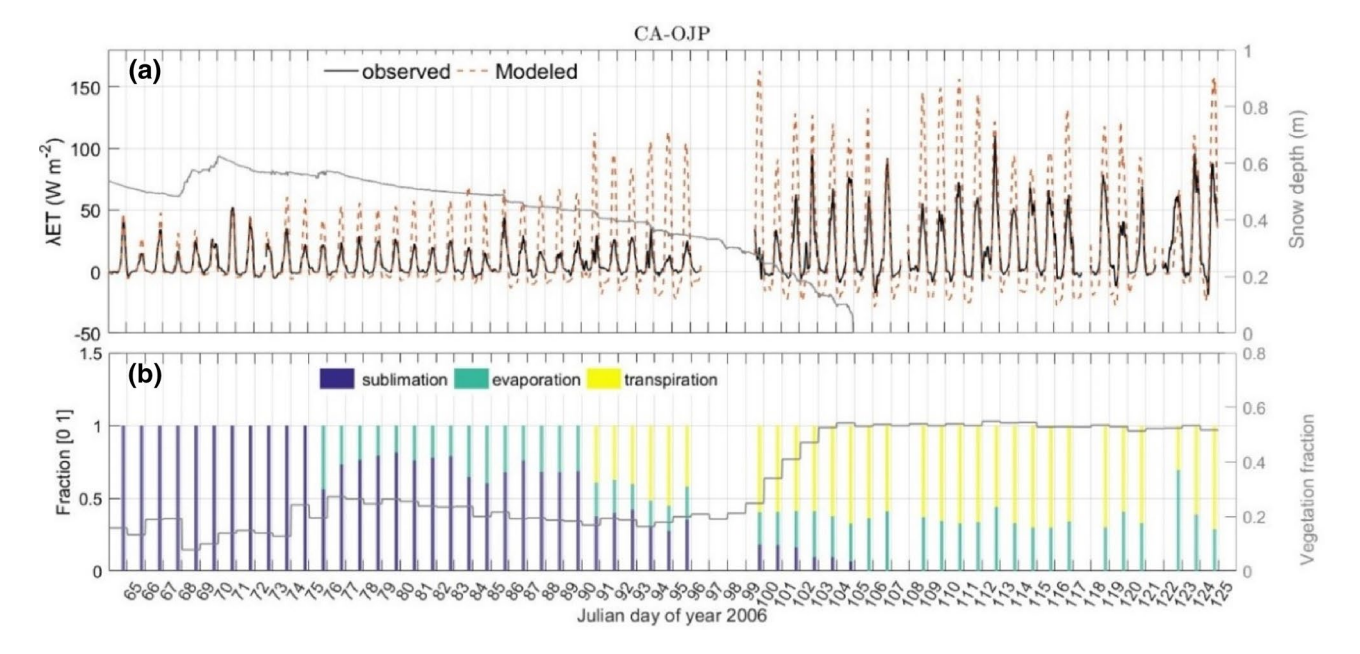


Figure 7. (a) MEP-ET modeled total ET. (b) Relative contribution of sublimation, evaporation, and transpiration to total ET assuming sublimation during snowmelt ($\beta = 1$ in Equation 4) and no constraint on the beginning of growing season (Equation 3 is used instead of Equation 8) at the CA-OJP site.

HAJJI ET AL. 12 of 20

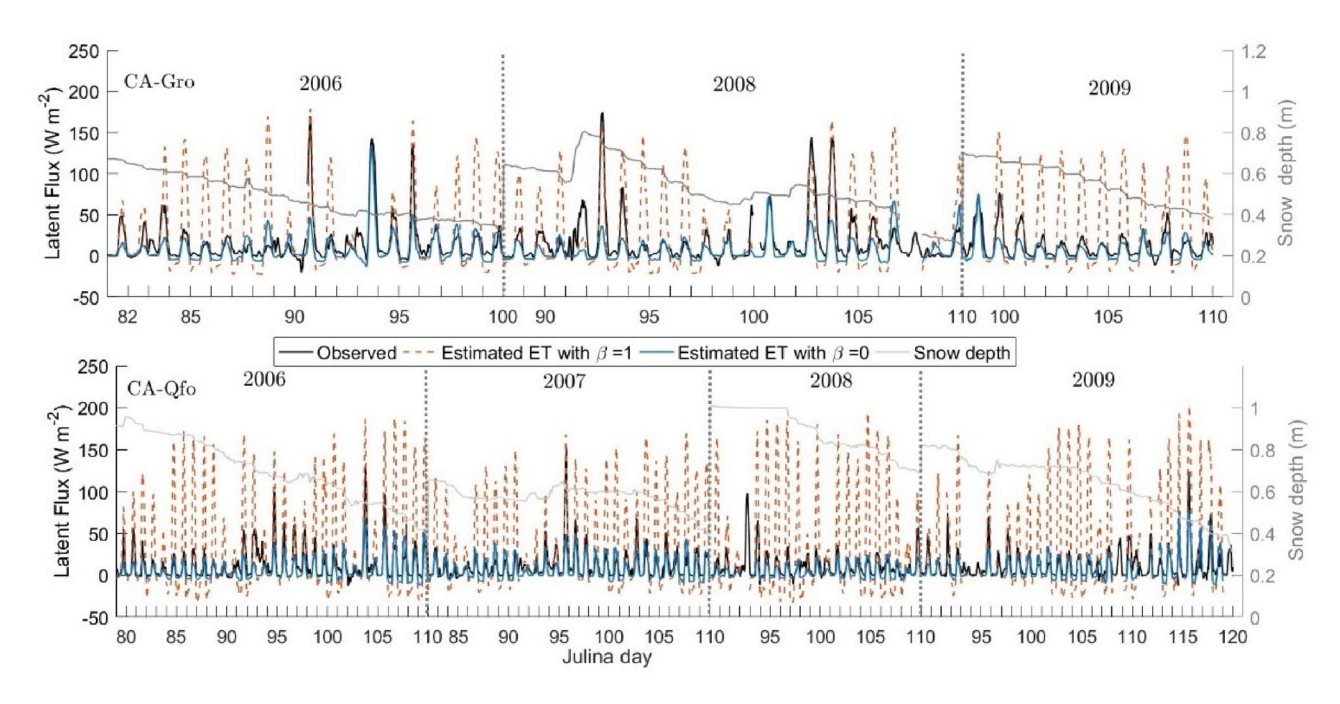


Figure 8. The MEP-ET with sublimation ($\beta = 1$ in Equation 4) versus the MEP-ET with no sublimation ($\beta = 0$ in Equation 4) compared with observed water vapor flux during snowmelt at the CA-Gro and CA-Qfo sites.

4.2.2. No Sublimation During Snowmelt ($\beta = 0$).

Figure 3b shows that the atmospheric vapor pressure tends to be lower than that right above the snow surface during the snow accumulation period, which makes sublimation possible. Sharply increasing atmospheric vapor pressures tend to suppress sublimation at the beginning of the snowmelt period. For snow sublimation to take place, the saturation-specific humidity above the snow surface needs to exceed the air-specific humidity above. Hence, the sublimation rates should decrease with snowmelt. This finding is consistent with earlier studies (Herrero & Polo, 2016; Ohta et al., 1993; Suzuki et al., 1999). A recent study of latent heat flux at the snow surface of the Sierra Nevadas in Spain showed that sublimation decreases sharply when snowmelt occurs (Herrero & Polo, 2016). They reported that sublimation accounted for about 50% of wintertime ablation (February), but only for about 12% in April and 4% in May.

Figures 8 and 9 show the MEP-ET water vapor flux with sublimation ($\beta=1$ in Equation 4) and without sublimation ($\beta=0$ during snowmelt period) compared with the observed latent heat flux at the four study sites. It is evident that the MEP-ET modeled latent heat flux with no sublimation agrees closely with the observed ET. The agreement is closer when the snow depth is higher as shown at the CA-Qfo and CA-Gro sites (Figure 8). This is due to the fact that the soil surface is less exposed when the snow depth is high. At these study sites, very short episodes of snowfall may occur during snowmelt. For example, snowfall was observed on the day of year 93-94-103-104 of year 2008 at the CA-Gro site, 96-104 of year 2006, and 96 of year 2007 at the CA-Qfo site. For these days, MEP-ET with sublimation ($\beta=1$ in Equation 4) is consistent with the observed ET since sublimation occurs over fresh snow with sub-freezing snow temperatures. If the snow temperature measurements are sufficiently accurate, the MEP-ET model can simulate sublimation during snowfall when the snow surface temperature is below the freezing point. Figure 8 indicates that the MEP-ET modeled ET is always in close agreement with the observations as long as the snow surface temperature data are accurate. The above analysis provides strong evidence for supporting the hypothesis that sublimation diminishes during snowmelt.

4.3. Vegetation Awakening

The MEP-ET model is capable of capturing the behavior of vegetation when it awakens and starts to transpire. Figures 6 and 7 show that the original MEP-ET overestimates water vapor flux not only during

HAJJI ET AL. 13 of 20

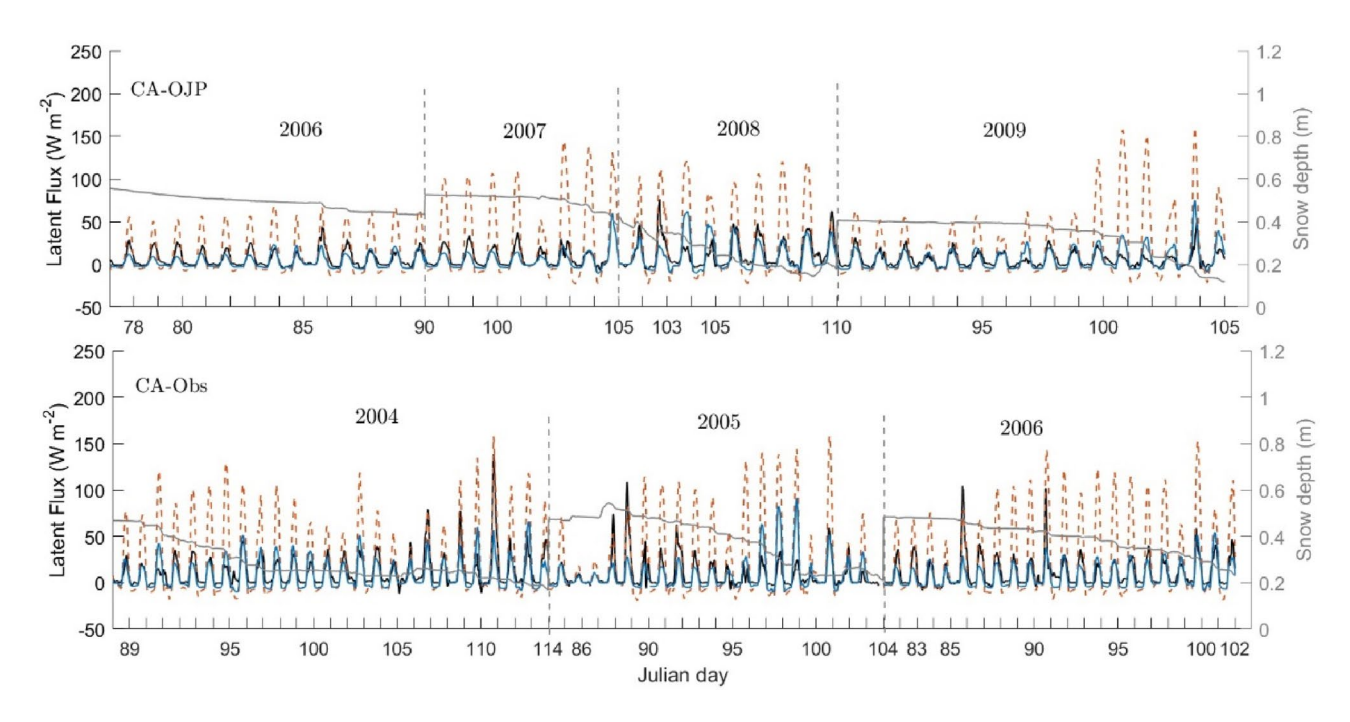


Figure 9. Same as Figure 8 for the CA-OJP and CA-Obs sites.

snowmelt (as discussed in the previous section) but also in the early stage of the growing season. Figure 10 shows simulated ET at the study sites using the revised MEP-ET model with a vegetation-awakening component, and no sublimation during snowmelt compared with the original MEP-ET model simulations. The simulated ET using the revised model is in much closer agreement with observations, especially during the three spring months when the temperature increases, snowmelt occurs, and vegetation activity progressively resumes after the dormant season. Note that the improved simulations of ET only occurred during the snowmelt and vegetation awakening periods.

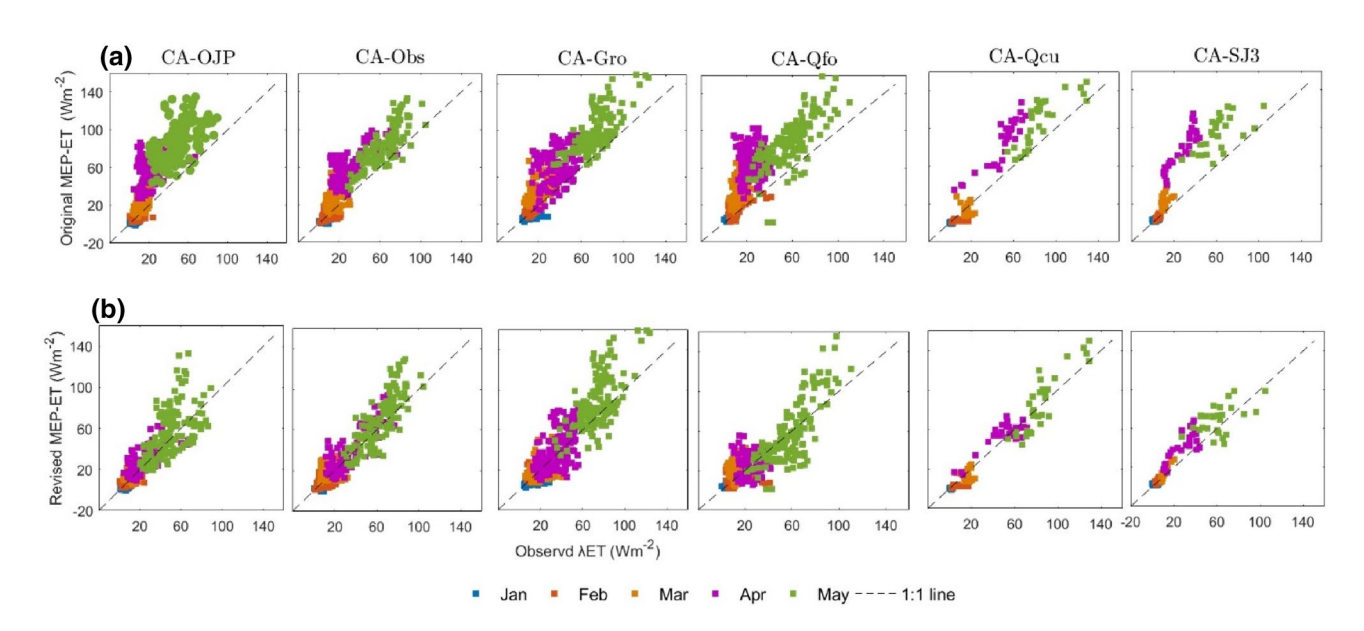


Figure 10. a) MEP ET with sublimation during snowmelt and no vegetation awakening correction versus observations at the study sites and (b) revised MEP ET with no sublimation during snowmelt and vegetation-awakening correction versus observations.

HAJJI ET AL. 14 of 20

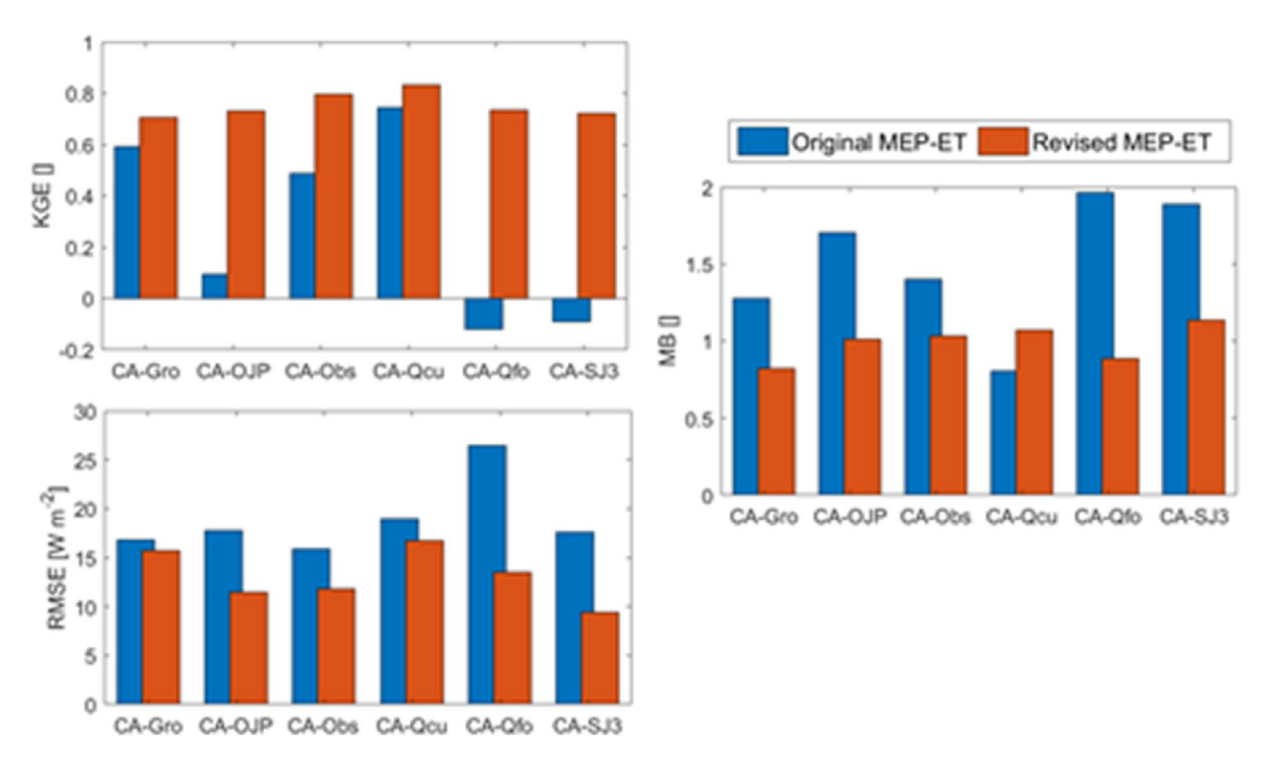


Figure 11. Performance values of the original and revised MEP-ET with statistics KGE, MB, and RMSE (W m⁻²) for critical seasons (snowmelt and early growing seasons) at the Canadian sites.

The performance scores of the revised MEP-ET model for the study sites are illustrated in Figure 11. KGE values range from 0.61 at CA-Gro to 0.83 at CA-Qcu and mean biases are low at all the study sites (~1). The MEP-ET model, with the two proposed revisions, can consistently simulate the total ET for the case of persistent snow cover (Figures 4 and 5) during the snowmelt and early spring dormant periods (Figure 6) under temperature stress conditions. Figure 12 presents a seasonal analysis of the original versus revised MEP-ET (boxplot) at the four study sites. The revised MEP-ET model, taking into account of sublimation and vegetation awakening, improves the ET estimation, especially for the snowmelt and canopy awakening months (March–May).

4.4. MEP-ET Model Partition of Available Energy

The partitioning of available energy in the MEP model is directly represented by the Bowen ratio (H/LE) according to Equation 3. Figure 13a, illustrating the estimated versus observed Bowen ratios over a 5-month period (January to May), clearly shows close agreement between the MEP and observed Bowen ratios. High Bowen ratios (>15) occurred in winter at some sites with cold temperatures and low latent heat fluxes. It has been reported that the Bowen ratio is expected to be much higher than one with substantial fluctuations when the air temperatures fall below 14°C (Andreas, 1989). Lower Bowen ratios, but still higher than those at the CA-Qcu site, are common at open sites with low air and surface temperatures and high albedos.

Differences between the estimated and observed Bowen ratios (Figure 13a) are more evident at some sites (CA-SJ3 and CA-Qcu) during the transition periods (April–May). This is in part caused by higher data uncertainties for the transition period, which lead to uncertainty in the Bowen ratio as a function of (q_s / T_s^2) according to the MEP model. Close correspondence between the observed and estimated Bowen ratios and between the Bowen ratios and air temperature and wind speed (Figures 13b and 13c) further confirm the performance of the revised MEP model. The MEP Bowen ratios tend to decrease with the air temperature. The highest Bowen ratios occurred at sub-freezing temperatures, consistent with previous studies. As winter progresses, latent heat fluxes increase with temperature and net radiation, leading to lower, but still greater than 1, Bowen ratios. As explained previously, canopy heating due to increasing sensible heat flux accelerates

HAJJI ET AL. 15 of 20

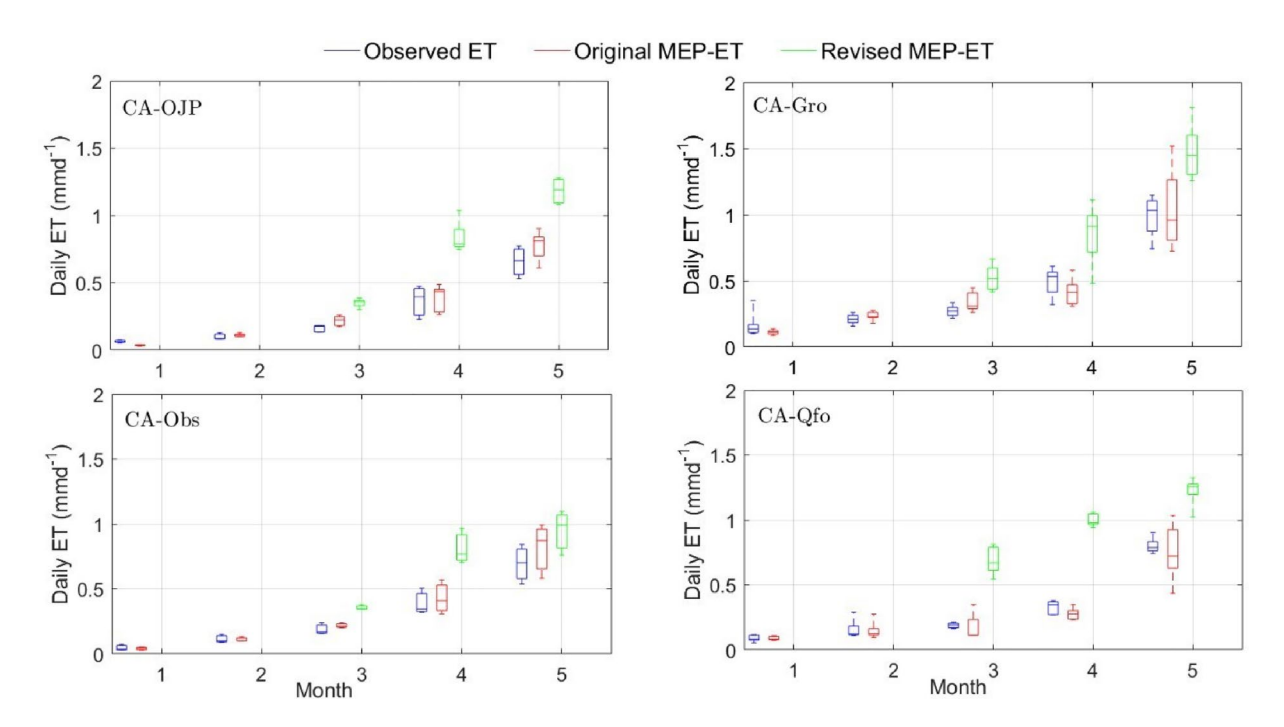


Figure 12. Seasonal analysis of the original versus revised MEP-ET.

melting, while sublimation diminishes it. At the beginning of the growing season, the above-freezing temperature allows transpiration, but low (air) temperature limits the transpiration rate leading to a high Bowen ratio. This behavioral change in the Bowen ratio is well captured by the revised MEP model. It should be emphasized that the MEP model is able to reproduce the observed relationship between the Bowen ratio and wind speed, even though the wind speed is not an input parameter to the MEP model (Figure 13c).

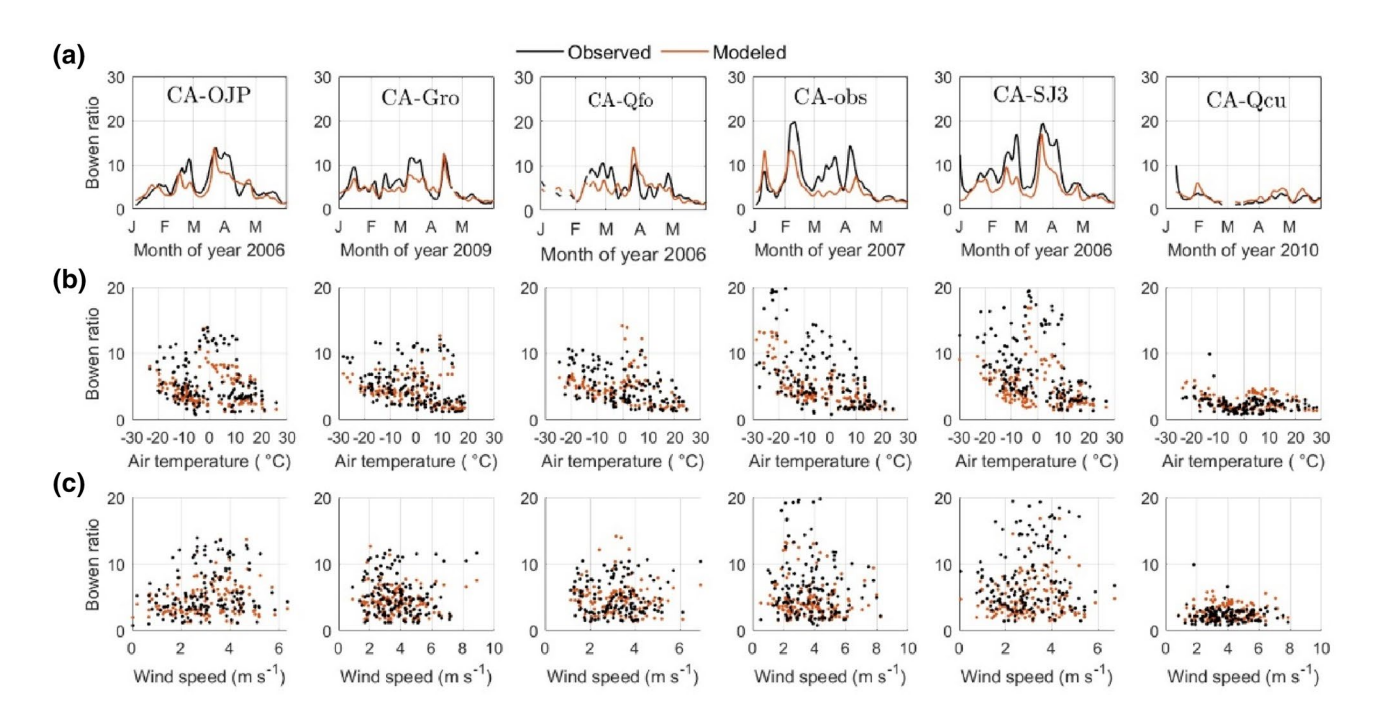


Figure 13. (a) Revised MEP versus observed Bowen ratio during the entire snow season (January–May); (b) Bowen ratios (observed: Bobs and estimated: Best) versus air temperature; and (c) wind speed over the same periods.

HAJJI ET AL. 16 of 20



5. Conclusion

This study tested and analyzed, for the first time, the capability of the MEP model for estimating water vapor fluxes over land surfaces with variable snow and vegetation cover during the winter-spring-summer transitions. The MEP-ET model performs well under these three critical periods characterizing the lifecycle of snowpacks: winter accumulation with growing snowpack, spring melting with isothermal snowpack, and spring-summer vegetation awakening when the growing season begins. During snow accumulation, the total water vapor loss is well captured by the MEP-ET model, at multiple sites and in consecutive years. A major finding of this study is that sublimation diminishes during snowmelt. The good performance of the MEP-ET model for seasonal snowpack results from parameterizing the effects of temperature stress on canopy transpiration and diminishing sublimation during snowmelt for heterogeneous land surfaces.

Data Availability Statement

All data sets used in this study are publicly available. Eddy covariance (EC) fluxes and meteorological variables were obtained from the FLUXNET network (http://daac.ornl.gov/FLUXNET/fluxnet.html).

Acknowledgments

This work was supported by the Ouranos Consortium on regional climatology and adaptation to climate change, Hydro-Québec, the Natural Sciences and Engineering Research Council of Canada, the MELCC, and Environment and Climate change Canada through project RDC-477125-14 entitled "Modélisation hydrologique avec bilan énergétique (ÉVAP)." Funding support is also provided by the NSF Polar Program Project 1724633. Partial support is provided by NASA NEWS Project NNX15AT41G and NSF CZO Project EAR-1331846.

References

Andreadis, K. M., Storck, P., & Lettenmaier, D. P. (2009). Modeling snow accumulation and ablation processes in forested environments. Water Resources Research, 45(5). https://doi.org/10.1029/2008wr007042

Andreas, E. L. (1989). Comments on "a physical bound on the Bowen ratio". *Journal of Applied Meteorology*, 28(11), 1252–1254. https://doi.org/10.1175/1520-0450(1989)028<1252:copbot>2.0.co;2

Arck, M., & Scherer, D. (2002). Problems in the determination of sensible heat flux over snow. *Geografiska Annaler–Series A: Physical Geography*, 84(3–4), 157–169.

Barlage, M., Chen, F., Tewari, M., Ikeda, K., Gochis, D., Dudhia, J., et al. (2010). Noah land surface model modifications to improve snow-pack prediction in the Colorado Rocky Mountains. *Journal of Geophysical Research*, 115(D22). https://doi.org/10.1029/2009jd013470

Beaty, C. B. (1975). Sublimation or melting: Observations from the white mountains, California and Nevada, USA. *Journal of Glaciology*, 14(71), 275–286.

Bengtsson, L. (1980). Evaporation from a snow cover: Review and discussion of measurements. Hydrology Research, 11(5), 221–234.

Bergh, J., & Linder, S. (1999). Effects of soil warming during spring on photosynthetic recovery in boreal Norway spruce stands. *Global Change Biology*, 5(3), 245–253.

Bernhardt, M., Liston, G. E., Strasser, U., Zängl, G., & Schulz, K. (2010). High resolution modelling of snow transport in complex terrain using downscaled MM5 wind fields. *The Cryosphere*, 4(1), 99. https://doi.org/10.5194/tc-4-99-2010

Betts, A. K. (2011). Seasonal climate transitions in New England. Weather, 66(9), 245-248.

Bernier, P. Y., & Swanson, R. H. (1993). The influence of opening size on snow evaporation in the forests of the Alberta Foothills. *Canadian Journal of Forest Research*, 23(2), 239–244. http://dx.doi.org/10.1139/x93-032

Boudhar, A., Boulet, G., Hanich, L., Sicart, J. E., & Chehbouni, A. (2016). Energy fluxes and melt rate of a seasonal snow cover in the Moroccan High Atlas. *Hydrological Sciences Journal*, 61(5), 931–943.

Brown, R. D., Brasnett, B., & Robinson, D. (2003). Gridded North American monthly snow depth and snow water equivalent for GCM evaluation. *Atmosphere-Ocean*, 41(1), 1–14.

Chen, B., Luo, S., Lii, S., Zhang, Y., & Ma, D. (2014a). Effects of the soil freeze-thaw process on the regional climate of the Qinghai-Tibet Plateau. Climate Research. 59(3), 243–257.

Chen, F., Barlage, M., Tewari, M., Rasmussen, R., Jin, J., Lettenmaier, D., et al. (2014b). Modeling seasonal snowpack evolution in the complex terrain and forested Colorado Headwaters region: A model intercomparison study. *Journal of Geophysical Research: Atmospheres*, 119(24), 13795–13819. https://doi.org/10.1002/2014jd022167

Clark, M. P., & Serreze, M. C. (2000). Effects of variations in East Asian snow cover on modulating atmospheric circulation over the North Pacific Ocean. *Journal of Climate*, 13(20), 3700–3710.

Dewar, R. C., Juretić, D., & Županović, P. (2006). The functional design of the rotary enzyme ATP synthase is consistent with maximum entropy production. *Chemical Physics Letters*, 430(1–3), 177–182.

 $De Walle, David\ R, \&\ Rango,\ Albert\ (2008).\ \textit{Principles of snow hydrolog},\ Cambridge\ University\ Press.$

Durand, Y., Giraud, G., Laternser, M., Etchevers, P., Mérindol, L., & Lesaffre, B. (2009). Reanalysis of 47 years of climate in the French Alps (1958–2005): Climatology and trends for snow cover. *Journal of Applied Meteorology and Climatology*, 48(12), 2487–2512.

Elliott, J. A., Toth, B. M., Granger, R. J., & Pomeroy, J. W. (1998). Soil moisture storage in mature and replanted sub-humid boreal forest stands. *Canadian Journal of Soil Science*, 78(1), 17–27. https://doi.org/10.4141/s97-021

Ensminger, I., Schmidt, L., & Lloyd, J. (2008). Soil temperature and intermittent frost modulate the rate of recovery of photosynthesis in Scots pine under simulated spring conditions. *New Phytologist*, 177(2), 428–442.

Essery, R., Morin, S., Lejeune, Y., & Ménard, C. B. (2013). A comparison of 1701 snow models using observations from an alpine site. Advances in Water Resources, 55, 131–148.

Essery, R., Rutter, N., Pomeroy, J., Baxter, R., Stähli, M., Gustafsson, D., & Elder, K. (2009). SNOWMIP2: An evaluation of forest snow process simulations. *Bulletin of the American Meteorological Society*, 90(8), 1120–1136.

Etchevers, P., Martin, E., Brown, R., Fierz, C., Lejeune, Y., Bazile, E., et al. (2004). Validation of the energy budget of an alpine snowpack simulated by several snow models (Snow MIP project). *Annals of Glaciology*, 38, 150–158.

Fang, X., & Pomeroy, J. W. (2007). Snowmelt runoff sensitivity analysis to drought on the Canadian prairies. Hydrological Processes: An International Journal, 21(19), 2594–2609.

HAJJI ET AL. 17 of 20



- Feng, X., Sahoo, A., Arsenault, K., Houser, P., Luo, Y., & Troy, T. J. (2008). The impact of snow model complexity at three CLPX sites. *Journal of Hydrometeorology*, 9(6), 1464–1481.
- Fitzpatrick, N., Radić, V., & Menounos, B. (2017). Surface energy balance closure and turbulent flux parameterization on a mid-latitude mountain glacier, Purcell Mountains, Canada. Frontiers in Earth Science, 5, 67. https://doi.org/10.3389/feart.2017.00067
- Franklin, O., Johansson, J., Dewar, R. C., Dieckmann, U., McMurtrie, R. E., Brännström Å., & Dybzinski, R. (2012). Modeling carbon allocation in trees: A search for principles. *Tree Physiology*, 32(6), 648–666.
- Ge, Y., & Gong, G. (2009). North American Snow Depth and Climate Teleconnection Patterns. Journal of Climate, 22(2), 217–233. https://doi.org/10.1175/2008jcli2124.1
- Golding, D. L., & Swanson, R. H. (1978). Snow accumulation and melt in small forest openings in Alberta. Canadian Journal of Forest Research. 8(4), 380–388.
- Gray, L. J. (1989). Emergence production and export of aquatic insects from a tallgrass prairie stream. *The Southwestern Naturalist*, 34(3), 313–318. https://doi.org/10.2307/3672158
- Groot Zwaaftink, C. D., Mott, R., & Lehning, M. (2013). Seasonal simulation of drifting snow sublimation in Alpine terrain. Water Resources Research, 49(3), 1581–1590.
- Gryning, S. E., Batchvarova, E., & De Bruin, H. A. R. (2001). Energy balance of a sparse coniferous high-latitude forest under winter conditions. *Boundary-Layer Meteorology*, 99(3), 465–488.
- Gupta, H. V., Kling, H., Yilmaz, K. K., & Martinez, G. F. (2009). Decomposition of the mean squared error and NSE performance criteria: Implications for improving hydrological modelling. *Journal of Hydrology*, 377(1–2), 80–91.
- Hajji, I., Nadeau, D. F., Music, B., Anctil, F., & Wang, J. (2018). Application of the maximum entropy production model of evapotranspiration over partially vegetated water-limited land surfaces. *Journal of Hydrometeorology*, 19(6), 989–1005.
- Harding, R. J. (1986). Exchanges of energy and mass associated with a melting snowpack. In E. M. Morris (Ed.), Modelling snowmelt-induced processes (pp. 3–15). IAHS Publication.
- Harding, R. J., & Pomeroy, J. W. (1996). The energy balance of the winter boreal landscape. Journal of Climate, 9(11), 2778–2787.
- Hayashi, M., Hirota, T., Iwata, Y., & Takayabu, I. (2005). Snowmelt energy balance and its relation to foehn events in Tokachi, Japan. Journal of the Meteorological Society of Japan. Ser. II, 83(5), 783–798.
- Herrero, J., Polo, M. J., & Eugster, W. (2016). Evaposublimation from the snow in the Mediterranean mountains of Sierra Nevada (Spain). The Cryosphere, 10(6), 2981–2998. https://doi.org/10.5194/tc-10-2981-2016
- Herrero, J., Polo, M. J., Moñino, A., & Losada, M. A. (2009). An energy balance snowmelt model in a Mediterranean site. *Journal of Hydrology*, 371(1-4), 98-107.
- Hetherington, E. D. (1987). The importance of forests in the hydrological regime. In M. C. Healey & R. R. Wallace (Ed.), Canadian aquatic resources. (pp. 179–211). Ottawa, ON: Department of Fisheries and Oceans.
- Hood, E., Williams, M., & Cline, D. (1999). Sublimation from a seasonal snowpack at a continental, mid-latitude alpine site. *Hydrological Processes*, 13(12–13), 1781–1797.
- Jackson, S. I., & Prowse, T. D. (2009). Spatial variation of snowmelt and sublimation in a high-elevation semi-desert basin of western Canada. *Hydrological Processes: An International Journal*, 23(18), 2611–2627.
- Jepsen, S. M., Molotch, N. P., Williams, M. W., Rittger, K. E., & Sickman, J. O. (2012). Interannual variability of snowmelt in the Sierra Nevada and Rocky Mountains, United States: Examples from two alpine watersheds. Water Resources Research, 48(2). https://doi.org/10.1029/2011wr011006
- Jin, H., Zhao, L., Wang, S., & Jin, R. (2006). Thermal regimes and degradation modes of permafrost along the Qinghai-Tibet Highway. Science in China - Series D: Earth Sciences, 49(11), 1170–1183.
- Kattelmann, R., & Elder, K. (1991). Hydrologic characteristics and water balance of an alpine basin in the Sierra Nevada. Water Resources Research, 27(7), 1553–1562.
- Kelly, A. E., & Goulden, M. L. (2016). A montane Mediterranean climate supports year-round photosynthesis and high forest biomass. Tree Physiology, 36(4), 459–468.
- Kozlowski, T. T., Kramer, P. J., & Pallardy, S. G. (1991). In The physiological ecology of woody plants, (Vol. 8, p. 213) Academic Press. https://doi.org/10.1093/treephys/8.2.213
- Kramer, P. J., & Boyer, J. S. (1995). Water relations of plants and soils. Academic Press.
- Kuusisto, E. (1986). The energy balance of a melting snow cover in different environments. IAHS Publication, 155, 37-45.
- Langer, M., Westermann, S., Muster, S., Piel, K., & Boike, J. (2011). The surface energy balance of a polygonal tundra site in northern Siberia Part 1: Spring to fall. *The Cryosphere*, 5, 151–171.
- Lee, Y. H., & Mahrt, L. (2004). An evaluation of snowmelt and sublimation over short vegetation in land surface modelling. *Hydrological Processes*, 18(18), 3543–3557.
- Lehning, M., & Katul, G. (2013). Snow-atmosphere interactions and hydrological consequences. *Advances in Water Resources*, 55, 1–3. https://doi.org/10.1016/j.advwatres.2013.02.001
- Lehning, M., Völksch, I., Gustafsson, D., Nguyen, T. A., Stähli, M., & Zappa, M. (2006). ALPINE3D: A detailed model of mountain surface processes and its application to snow hydrology. *Hydrological Processes: An International Journal*, 20(10), 2111–2128.
- Link, T., & Marks, D. (1999). Distributed simulation of snowcover mass-and energy-balance in the boreal forest. *Hydrological Processes*, 13(14–15), 2439–2452.
- Liston, G. E. (2004). Representing subgrid snow cover heterogeneities in regional and global models. *Journal of Climate*, 17(6), 1381–1397. Liston, G. E., & Elder, K. (2006). A distributed snow-evolution modeling system (SnowModel). *Journal of Hydrometeorology*, 7(6), 1259–1276.
- Liu, X., Nie, Y., Luo, T., Yu, J., Shen, W., & Zhang, L. (2016). Seasonal shift in climatic limiting factors on tree transpiration: Evidence from sap flow observations at alpine treelines in southeast Tibet. Frontiers of Plant Science, 7, 1018.
- Lorenz, R. D., Lunine, J. I., Withers, P. G., & McKay, C. P. (2001). Titan, Mars and Earth: Entropy production by latitudinal heat transport. Geophysical Research Letters, 28(3), 415–418. https://doi.org/10.1029/2000gl012336
- MacDonald, M. K., Pomeroy, J. W., & Pietroniro, A. (2010). On the importance of sublimation to an alpine snow mass balance in the Canadian Rocky Mountains. *Hydrology and Earth System Sciences*, 14(7), 1401.
- Magnusson, J., Wever, N., Essery, R., Helbig, N., Winstral, A., & Jonas, T. (2015). Evaluating snow models with varying process representations for hydrological applications. *Water Resources Research*, 51(4), 2707–2723.
- Malkus, W. V. (2003). Borders of disorder: In turbulent channel flow. Journal of Fluid Mechanics, 489, 185-198.
- Marks, D., Dozier, J., & Davis, R. E. (1992). Climate and energy exchange at the snow surface in the alpine region of the Sierra Nevada: 1. Meteorological measurements and monitoring. *Water Resources Research*, 28(11), 3029–3042.

HAJJI ET AL. 18 of 20



- Marks, D., Winstral, A., Flerchinger, G., Reba, M., Pomeroy, J., Link, T., & Elder, K. (2008). Comparing simulated and measured sensible and latent heat fluxes over snow under a pine canopy to improve an energy balance snowmelt model. *Journal of Hydrometeorology*, 9(6), 1506–1522.
- Marks, D., Winstral, A., & Seyfried, M. (2002). Simulation of terrain and forest shelter effects on patterns of snow deposition, snowmelt and runoff over a semi-arid mountain catchment. *Hydrological Processes*, 16(18), 3605–3626.
- Martinelli, M., Jr (1960). Moisture exchange between the atmosphere and alpine snow surfaces under summer conditions (preliminary results). *Journal of Meteorology*, 17(2), 227–231.
- Mellander, P. E., Bergh, J., Lundmark, T., & Bishop, K. (2008). Recovery of photosynthetic capacity in Scots pine: A model analysis of forest plots with contrasting soil temperature. *European Journal of Forest Research*, 127(1), 71–79.
- Mellander, P. E., Bishop, K., & Lundmark, T. (2004). The influence of soil temperature on transpiration: A plot scale manipulation in a young Scots pine stand. Forest Ecology and Management, 195(1–2), 15–28.
- Mellander, P. E., Stähli, M., Gustafsson, D., & Bishop, K. (2006). Modelling the effect of low soil temperatures on transpiration by Scots pine. *Hydrological Processes: An International Journal*, 20(9), 1929–1944.
- Molotch, N. P., Blanken, P. D., Williams, M. W., Turnipseed, A. A., Monson, R. K., & Margulis, S. A. (2007). Estimating sublimation of intercepted and sub-canopy snow using eddy covariance systems. *Hydrological Processes: An International Journal*, 21(12), 1567–1575.
- Monson, R. K., Sparks, J. P., Rosenstiel, T. N., Scott-Denton, L. E., Huxman, T. E., Harley, P. C., et al. (2005). Climatic influences on net ecosystem CO₂ exchange during the transition from wintertime carbon source to springtime carbon sink in a high-elevation, subalpine forest. *Oecologia*, 146(1), 130–147.
- Montesi, J., Elder, K., Schmidt, R. A., & Davis, R. E. (2004). Sublimation of intercepted snow within a subalpine forest canopy at two elevations. *Journal of Hydrometeorology*, 5(5), 763–773.
- Mott, R., Vionnet, V., & Grünewald, T. (2018). The seasonal snow cover dynamics: Review on wind-driven coupling processes. Frontiers in Earth Science, 6, 197.
- Mu, Q., Heinsch, F. A., Zhao, M., & Running, S. W. (2007). Development of a global evapotranspiration algorithm based on MODIS and global meteorology data. *Remote Sensing of Environment*. 111(4), 519–536.
- Nakai, Y., Sakamoto, T., Terajima, T., Kitamura, K., & Shirai, T. (1999). The effect of canopy-snow on the energy balance above a coniferous forest. *Hydrological Processes*, 13(14–15), 2371–2382.
- Niu, G. Y., & Yang, Z. L. (2007). An observation-based formulation of snow cover fraction and its evaluation over large North American river basins. *Journal of Geophysical Research: Atmospheres*, 112(D21). https://doi.org/10.1029/2007jd008674
- Ohta, T., Hashimoto, T., & Ishibashi, H. (1993). Energy budget comparison of snowmelt rates in a deciduous forest and an open site. *Annals of Glaciology*, 18, 53–59.
- Ozawa, H., Shimokawa, S., & Sakuma, H. (2001). Thermodynamics of fluid turbulence: A unified approach to the maximum transport properties. *Physical Review E*, 64(2), 026303.
- Paltridge, G. W. (1978). The steady-state format of global climate. *Quarterly Journal of the Royal Meteorological Society*, 104(442), 927–945. Parviainen, J., & Pomeroy, J. W. (2000). Multiple-scale modelling of forest snow sublimation: Initial findings. *Hydrological Processes*, 14(15), 2669–2681.
- Pomeroy, J. W., & Essery, R. L. H. (1999). Turbulent fluxes during blowing snow: Field tests of model sublimation predictions. *Hydrological Processes*, 13(18), 2963–2975.
- Pomeroy, J. W. & Granger, R. J. (1997). Sustainability of the western canadian boreal forest under changing hydrological conditions. I. snow accumulation and ablation. In D. Rosjberg, N. Boutayeb, A. Gustard, Z. Kundzewicz & P. Rasmussen (Eds.), Sustainability of Water Resources Under Increasing Uncertainty, (Vol. 240, pp. 237–242). Wallingford, UK: International Association of Hydrological Sciences.
- Prueger, J. H., Hatfield, J. L., & Sauer, T. J. (1998). Surface energy balance partitioning over rye and oats cover crops in central Iowa. *Journal of Soil and Water Conservation*, 53(3), 263–268.
- Radic, V., Menounos, B., Shea, J., Fitzpatrick, N., Tessema, M. A., & Déry, S. J. (2017). Evaluation of different methods to model near-surface turbulent fluxes for a mountain glacier in the Cariboo Mountains, BC, Canada. *The Cryosphere*, 11(6), 2897–2918. https://doi.org/10.5194/tc-11-2897-2017
- Reba, M. L., Pomeroy, J., Marks, D., & Link, T. E. (2012). Estimating surface sublimation losses from snowpacks in a mountain catchment using eddy covariance and turbulent transfer calculations. *Hydrological Processes*, 26(24), 3699–3711.
- Repo, T., Mononen, K., Alvila, L., Pakkanen, T. T., & Hänninen, H. (2008). Cold acclimation of pedunculate oak (*Quercus robur* L.) at its northernmost distribution range. *Environmental and Experimental Botany*, 63(1–3), 59–70.
- Rutter, N., Essery, R., Pomeroy, J., Altimir, N., Andreadis, K., Baker, I., et al. (2009). Evaluation of forest snow processes models (Snow-MIP2). *Journal of Geophysical Research*, 114(D6). https://doi.org/10.1029/2008jd011063
- Sade, R., Rimmer, A., Litaor, M. I., Shamir, E., & Furman, A. (2014). Snow surface energy and mass balance in a warm temperate climate mountain. *Journal of Hydrology*, 519, 848–862.
- Schlögl, S., Lehning, M., Nishimura, K., Huwald, H., Cullen, N. J., & Mott, R. (2017). How do stability corrections perform in the stable boundary layer over snow?. *Boundary-Layer Meteorology*, 165(1), 161–180.
- Schulz, O., & De Jong, C. (2004). Snowmelt and sublimation: Field experiments and modelling in the high Atlas Mountains of Morocco. Hydrology and Earth System Sciences, 8(6), 1076–1089. https://doi.org/10.5194/hess-8-1076-2004
- Schwarz, P. A., Fahey, T. J., & Dawson, T. E. (1997). Seasonal air and soil temperature effects on photosynthesis in red spruce (*Picea rubens*) saplings. *Tree Physiology*, 17(3), 187–194.
- Schmidt, R A, Troendle, C A, & Meiman, J R (1998). Sublimation of snowpacks in subalpine conifer forests. *Canadian Journal of Forest Research*, 28(4), 501–513. http://dx.doi.org/10.1139/x98-033
- Sexstone, G. A., Clow, D. W., Stannard, D. I., & Fassnacht, S. R. (2016). Comparison of methods for quantifying surface sublimation over seasonally snow-covered terrain. *Hydrological Processes*, 30(19), 3373–3389.
- Shanafield, M., Cook, P. G., Gutiérrez-Jurado, H. A., Faux, R., Cleverly, J., & Eamus, D. (2015). Field comparison of methods for estimating groundwater discharge by evaporation and evapotranspiration in an arid-zone playa. *Journal of Hydrology*, 527, 1073–1083.
- Slater, A. G., Schlosser, C. A., Desborough, C. E., Pitman, A. J., Henderson-Sellers, A., Robock, A., et al. (2001). The representation of snow in land surface schemes: Results from PILPS 2 (d). *Journal of Hydrometeorology*, 2(1), 7–25.
- Stewart, I. T., Cayan, D. R., & Dettinger, M. D. (2004). Changes in snowmelt runoff timing in western North America under a business as usual climate change scenario. Climatic Change, 62(1–3), 217–232.
- Stiegler, C., Lund, M., Christensen, T. R., Mastepanov, M., & Lindroth, A. (2016). Two years with extreme and little snowfall: Effects on energy partitioning and surface energy exchange in a high-Arctic tundra ecosystem. *The Cryosphere*, 10(4).

HALII ET AL. 19 of 20

in Meteorology, 2015, 1-12. https://doi.org/10.1155/2015/286206



- Strasser, U., Bernhardt, M., Weber, M., Liston, G. E., & Mauser, W. (2008). Is snow sublimation important in the alpine water balance?. *The Cryosphere*, 2, 53–66.
- Su, H., Yang, Z. L., Niu, G. Y., & Dickinson, R. E. (2008). Enhancing the estimation of continental-scale snow water equivalent by assimilating MODIS snow cover with the ensemble Kalman filter. *Journal of Geophysical Research*, 113(D8). https://doi.org/10.1029/2007jd009232 Suzuki, K., Liston, G. E., & Matsuo, K. (2015). Estimation of continental-basin-scale sublimation in the Lena river basin, Siberia. *Advances*
- Suzuki, K., Ohta, T., Kojima, A., & Hashimoto, T. (1999). Variations in snowmelt energy and energy balance characteristics with larch forest density on Mt Iwate, Japan: Observations and energy balance analyses. *Hydrological Processes*, 13(17), 2675–2688.
- Svoma, B. M. (2016). Difficulties in Determining Snowpack Sublimation in Complex Terrain at the Macroscale. *Advances in Meteorology*, 2016, 1–10. http://dx.doi.org/10.1155/2016/9695757
- Turnipseed, A. A., Anderson, D. E., Blanken, P. D., Baugh, W. M., & Monson, R. K. (2003). Airflows and turbulent flux measurements in mountainous terrain: Part 1. Canopy and local effects. *Agricultural and Forest Meteorology*, 119(1–2), 1–21.
- Turnipseed, A. A., Blanken, P. D., Anderson, D. E., & Monson, R. K. (2002). Energy budget above a high-elevation subalpine forest in complex topography. *Agricultural and Forest Meteorology*, 110(3), 177–201.
- Van den Broeke, M., Smeets, P., Ettema, J., Van der Veen, C., Van de Wal, R., & Oerlemans, J. (2008). Partitioning of melt energy and meltwater fluxes in the ablation zone of the west Greenland ice sheet. *The Cryosphere*, 2(2), 179. https://doi.org/10.5194/tc-2-179-2008
- Wang, J., & Bras, R. L. (2011). A model of evapotranspiration based on the theory of maximum entropy production. Water Resources Research, 47(3). https://doi.org/10.1029/2010wr009392
- Wang, J., Bras, R. L., Nieves, V., & Deng, Y. (2014). A model of energy budgets over water, snow, and ice surfaces. *Journal of Geophysical Research: Atmospheres*, 119(10), 6034–6051.
- Wang, Y., Mao, Z., Bakker, M. R., Kim, J. H., Brancheriau, L., Buatois, B., et al. (2018). Linking conifer root growth and production to soil temperature and carbon supply in temperate forests. *Plant and Soil*, 426(1–2), 33–50.
- Wang, H., Tetzlaff, D., & Soulsby, C. (2017). Testing the maximum entropy production approach for estimating evapotranspiration from closed canopy shrubland in a low-energy humid environment. *Hydrological Processes*, 31(25), 4613–4621.
- Wang, J., Bras R. L., Sivandran, G., & Knox, R. G. (2010). A simple method for the estimation of thermal inertia. *Geophysical Research Letters*, 37(5). http://dx.doi.org/10.1029/2009gl041851
- Wang, S., Yang, Y., Luo, Y., & River, A. (2013). Spatial and seasonal variations in evapotranspiration over Canada's landmass. *Hydrology and Earth System Sciences Discussions*, 10(5), 6107–6151. http://dx.doi.org/10.5194/hessd-10-6107-2013
- Wieser, G., & Tausz, M.(Eds.), (2007). Trees at their upper limit: Treelife limitation at the alpine timberline. Dordrecht, The Netherlands: Springer.
- Winchell, T. S. (2016). Changing snowpack dynamics: Phase predictions and forest implications. Doctoral dissertation, University of Colorado at Boulder.
- Wittich, K. P., & Hansing, O. (1995). Area-averaged vegetative cover fraction estimated from satellite data. *International Journal of Biometeorology*, 38(4), 209–215.
- Xu, L., & Dirmeyer, P. (2011). Snow-atmosphere coupling strength in a global atmospheric model. *Geophysical Research Letters*, 38(13). https://doi.org/10.1029/2011gl048049
- Zhang, Y., Ishikawa, M., Ohata, T., & Oyunbaatar, D. (2008). Sublimation from thin snow cover at the edge of the Eurasian cryosphere in Mongolia. *Hydrological Processes: An International Journal*, 22(18), 3564–3575.
- Zhang, Y., Suzuki, K., Kadota, T., & Ohata, T. (2004). Sublimation from snow surface in southern mountain taiga of eastern Siberia. *Journal of Geophysical Research*, 109(D21). https://doi.org/10.1029/2003jd003779
- Zhou, H. F., Zheng, X. J., Zhou, B., Dai, Q., & Li, Y. (2012). Sublimation over seasonal snowpack at the southeastern edge of a desert in central Eurasia. *Hydrological Processes*, 26(25), 3911–3920.

HAJJI ET AL. 20 of 20